Nanosecond Pulse Breakdown of Gas-Insulated Gaps

1990

Yukimitsu Kawada

Nanosecond Pulse Breakdown of Gas-Insulated Gaps

(ナノセカンド・パルスに依る各種気体の絶縁破壊に関する研究)

Yukimitsu Kawada

Department of Electrical and Computer Engineering,

Nagoya Institute of Technology

To my father in heaven and my family

There are more things in heaven and earth, Kawada,

Than are dreamt of in your philosophy.

CONTENTS

Preface a

Chapter I Development and Waveform Analysis of a Coaxial-type Marx Generator

1 Introduction 2

2 Element configulation of the CMG 4

3 Measurements of ns impulse voltage 7

4 Waveform analysis of the coaxial-type Marx generator 9

5 Results of calculation 14

6 Improvement of waveform 24

6.1 Improvement of rise time 24

6.2 Reduction of pulse duration 26

6.3 Reduction of harmonics 27

7 Investigation of output impulse voltage waveforms 27

8 Measurement of ns current pulse 30

8.1 Observation of ns current pulse 34

9 Conclusions 38

References 39

Chapter II Nanosecond Pulse Breakdown of Gas-Insulated Gaps

1 Introduction 42

2 Apparatus 46

3 Experimental Results 48

4 Discussion 59

4.1 Validity of Paschen's law 59

4.2 Investigation of the breakdown mechanism 62

5 Conclusions 66

References 68

Chapter III Breakdown Phenomena of Gas-Insulated Gaps With Nanosecond Pulses

1	Introduction	71
2	Apparatus	73
3	Experimental Results	77
3.1	50% probability of flashover voltage	77
3.2	Observed time lag of flashover	85
4	Discussion	100
5	Conclusions	102
References		104

Chapter IV Observation of Nanosecond Pulse Breakdown of Gas-Insulated Gaps by Image Converter Camera

1	Introduction	106
2	Apparatus	112
3	Experimental Results	115

4 Discussion 123

5 Conclusions 125

References 127

Chapter V Conclusions 129

Acknowldgment 135

List of articles published 137

Preface

Many research works on breakdown mechanism of gaseous discharge have been carried out. In the regime where $p\ell$ (p: pressure, ℓ : gap length) and overvoltage ratio are low, Townsend's theory may be applicable. Streamer theory by Loeb, Meek and Raether is dominant in the regime of high $p\ell$ and high overvoltage ratio. Although electron emission from the cathode is, of course, required to establish flashover, the main difference from Townsend's theory generation mechanism is that a discharge with a velocity of the order of 10^7-10^8 cm/s, can develop regardless of γ (electron emission from cathode by secondary mechanism) at the beginning of breakdown dominated by applied static field. This is an essential difference between Townsend's theory and streamer theory. The regime of validity of these models, however, is not clear because of their complexity.

On the other hand, it is generally understood that impulse voltage breakdown shows different properties depending on rise time and pulse duration. This is due to the fact that transition process from an electron avalanche to a streamer and its development are influenced

by the applied field and duration. The drift velocity of the electrons, the space charge field ahead of an electron avalanche, and the residual positive ion group seem to be strongly involved with the transition.

Breakdown phenomena of gas-insulated gaps, obtained with nanosecond pulse, have already been reported by Kunhardt and Byszewski and they have explained the development of a streamer by a runaway electron model . In the transition process from an electron avalanche to a streamer, considering mutual actions by space charge field due to a group of electrons ahead of electron avalanche and applied field of the gap, the author agrees with the physical possibility of such electrons. Namely, one electron emitted from the cathode develops into a gap in forming the avalanche. The electrons produced by ionization of collisions are located ahead of the electron avalanche. The movement of the positive ions is short in comparison with the drift velocity of electrons so that the positive ions are considered to stand still where they are produced.

Therefore, only positive ions stand in line along the avalanche path and, moreover, the maximum density of positive ions occurs next to the group of electrons ahead of the avalanche. The electrons are

retarded by these ion groups. This retarding force strongly increases with development of the avalanche. The electrons actually stop advancing at a certain distance. At this stage, the electrons are more strongly attracted by positive ions and conversion into plasma with high conductivity occurs. In this transition process from an avalanche to a streamer and the streamer development under the ultrahigh-field, runaway electrons are considered to the electrons ejected from the avalanche head. Theoretical and experimental approaches have been carried out by many researchers to investigate the breakdown mechanism initiated with the runaway electrons by using nanosecond pulses. These articles, however, do not mention about $p\ell$ vs. flashover characteristics nor breakdown luminosity of a gas in the gap of the gaseous discharge. For the purpose of clarifying the streamer formation and its development, and the breakdown mechanism of the gaseous dicharge, an examination of $p\ell$ vs. flashover characteristics, time lag characteristics and streamer developing phenomena was carried out under the application of nanosecond pulses, which were generated by the coaxial-type Marx generator.

As a result of the investigation, the author found that the breakdown mechanism due to the application of the nanosecond pulses

could be explained by the conventional avalanche-to-streamer development theory. This doctoral dissertation shows the investigation of the breakdown mechanism in addition to waveform analysis of the Marx generator.

Nanosecond Pulse Breakdown of Gas-Insulated Gaps

（ナノセカンド・パルスに依る各種気体の絶縁破壊に関する研究）

Yukimitsu Kawada

Department of Electrical and Computer Engineering,

Nagoya Institute of Technology

Chapter I Development and waveform analysis of a Coaxial-Type Marx Generator*

1 Introduction

Impulses for power engineering such as lightning and switching impulses can be generated by a so called Marx generator with n stages. It is well known that the waveform may be expressed by an output voltage from an equivalent circuit with concentrated constants, L, C and R.

On the other hand, in recent years, a coaxial-type Marx generator (hereafter called CMG) has been developed as a source of relativistic electron beams and laser pumping apparatus in the field of nuclear fusion. The output voltage from CMG forms nanosecond pulses. The equivalent circuit can be represented by the distributed constant circuits with n stages, whose

* Submitted to Journal of Physics E: Scientific Instruments for review

each stage forms a module.[1-4]

The author has already examined nanosecond pulse breakdown of gas insulated gaps by using the CMG and investigated the breakdown mechanism from the behavior of electrons and streamers.[5-7] It led to the conclusion that the breakdown mechanism in the ultrahigh field region, subjected to nanosecond pulses with a rise time of 10.8 ns and pulse duration at half-peak of 30 ns may be explained by the conventional avalanche-to-streamer development theory.

In this article, the equivalent circuit of the CMG used in this examination is represented by the distributed constant circuits and the waveform analysis was aided by a computer. Moreover, it was clarified that it was possible to obtain megavolt impulses by selecting elements with appropriate values in each stage.

The author also examined the methods of impulse voltage and current measurements, and $CuSO_4$ solution resistance divider and coaxial type resistance divider, and pick-up coil with one turn enabled the author to measure the impulse voltage and current, respectively.

This research paper indicates the waveform analysis of the coaxial-type Marx generator and measurements of impulse voltage and current.

2 Element configulation of the CMG

The element configulation of the CMG is shown in Fig.1 and the unit module of the CMG .is illustrated in Fig.2. The CMG consists of 6 stages of modules. Each module is connected in series and is installed inside the stainless container, filled with oil. Each module is designed in a coaxial type and is designed to decrease the circuit constants as possible as could to obtain the desired waveform with the sharp rise time of the generated voltage. All spark gaps are installed along the central axis of the CMG to obtain low jitter switching of the spark gaps. The installment of the spark gaps enables the ultraviolet rays, generated at the first spark gap to irradiate the surface of other spark gaps so that the triggering characteristics with low jitter can be obtained. Pre-breakdown generated by Thyratron pulser (so called Trigatron gap system) initiates the main flashover across the gaps of

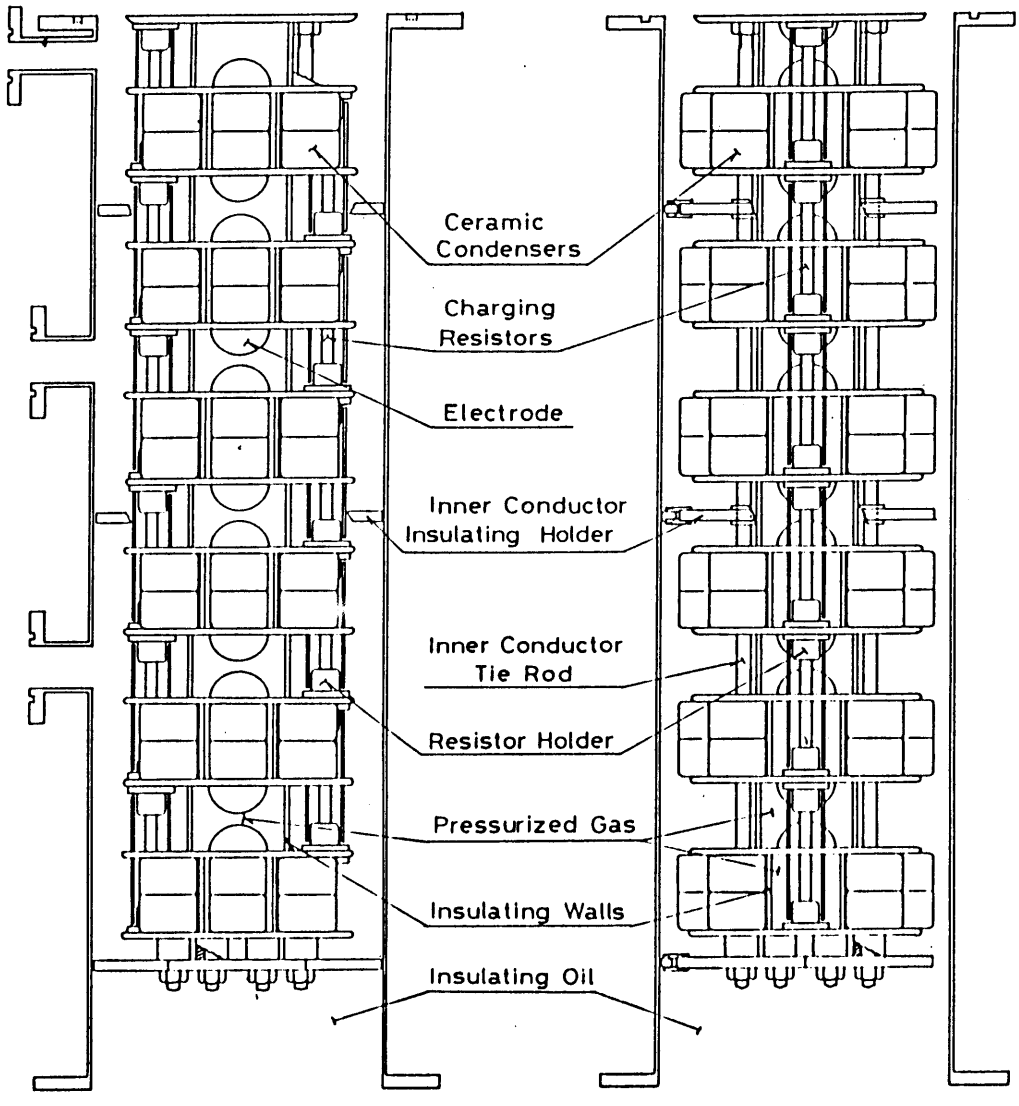

Fig. 1 Layout of the elements in CMG (viewed from two different cross sections)

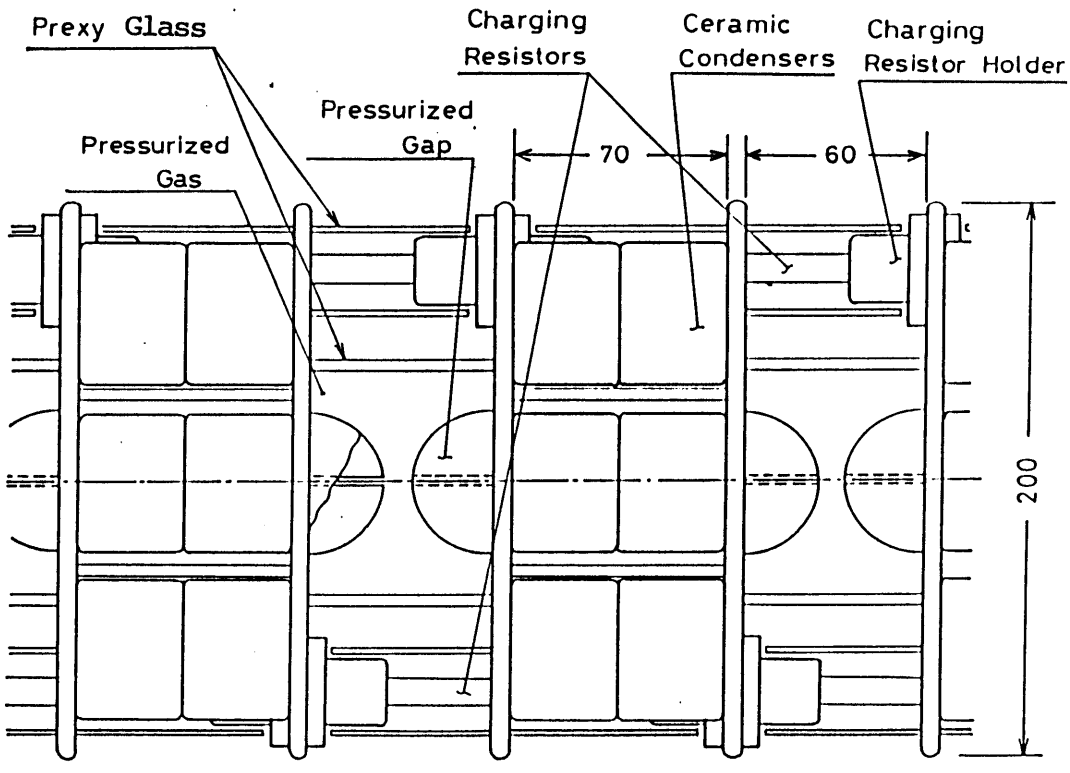

Fig. 2 Layout of the elements in unit module of CMG

the first stage, which can produce the full sparking of the second through the sixth stage of gaps by a flashover.

3 Measurement of ns impulse voltage

The schematic diagram for measuring ns impulse voltages is shown in Fig.3. The output voltages can be reduced through both a coaxial $CuSO_4$ solution resistance divider and coaxial resistance dividers, connected in series and can be detected by an oscilloscope. All connecting coaxial cables with characteristic impedance, 50 ohms are placed inside copper tubes to minimize the electrical noise. The oscilloscope was installed inside a Faraday cage made of copper plates. Divider ratio of each resistance divider was measured by an oscilloscope with help of high frequency pulse generator (Hewlett Packard Co.). A total of the divider ratio of the whole circuit was also measured by the same way and was confirmed that there was no discrepancy between the measured values. It was also confirmed that the response time of the measuring circuit was less than 1 ns.

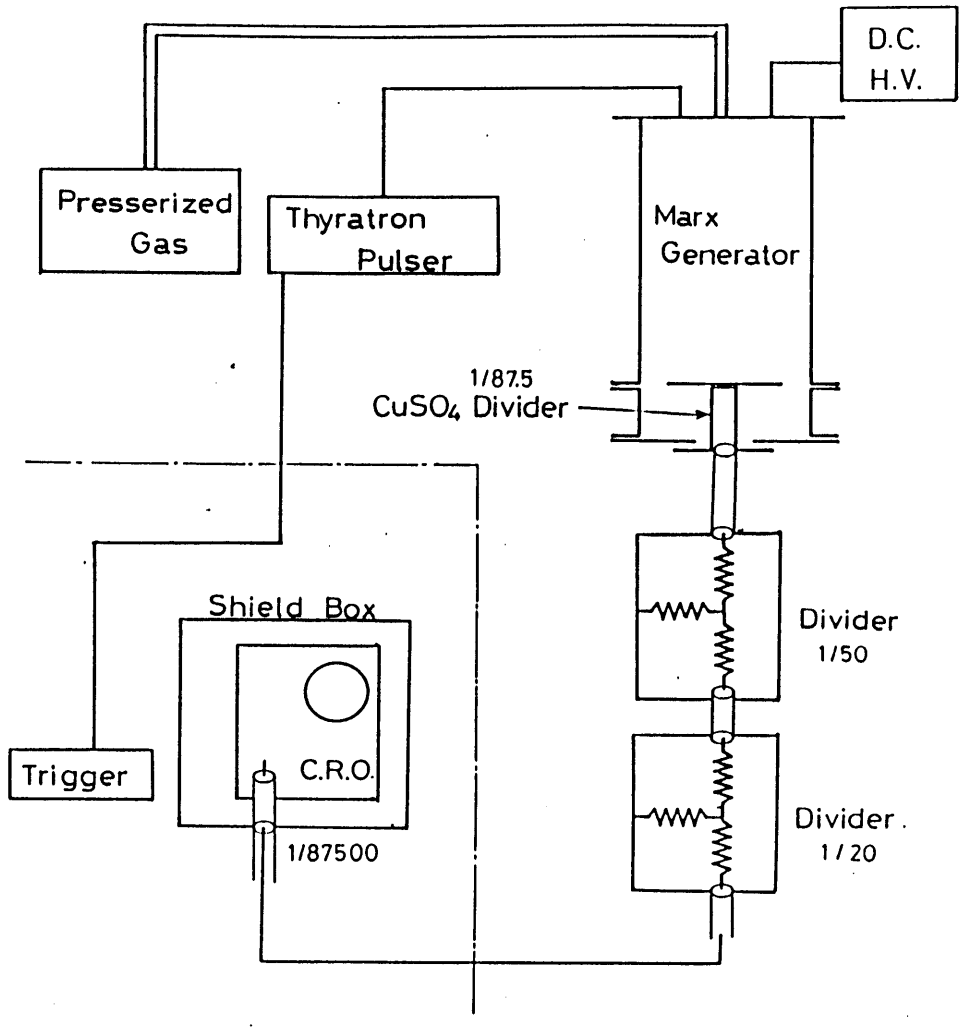

Fig. 3 The voltage measurement circuit

An impulse waveform obtained in this test is shown in Fig.4. Rise times of 10.8 ns and pulse duration at half peak of 30 ns are obtained.

4 Waveform analysis of the coaxial-type Marx generator

The equivalent circuit of the CMG with 6 stages, illustrated above is shown in Fig.5 . .

Each element is designated as follows,

R: Internal resistance of a charging capacitor plus a resistance in a unit module

R_0: Coaxial output resistance ($CuSO_4$ solution)

R_a: Streamer's resistance across the spark gaps

L: Internal inductance existed in each module

L_a: Streamer's inductance across the spark gaps

L_e: Inductance in the last stage,with output terminals

L_0: Internal inductance of the coaxial output resistance

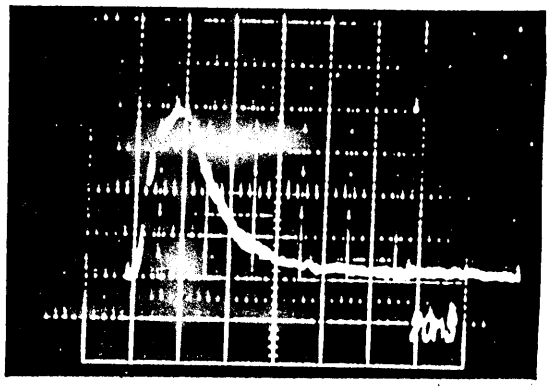

Fig. 4 Impulse waveform

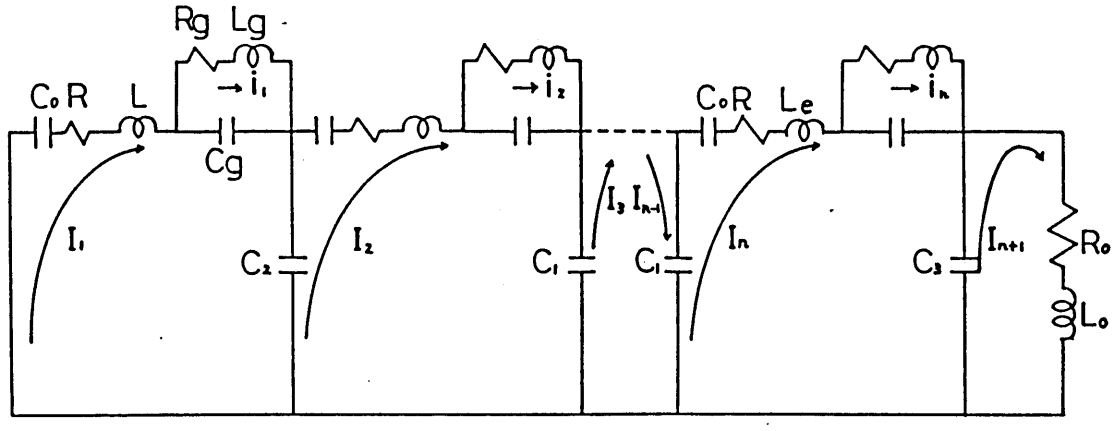

Fig. 5 The equivalent circuit of CMG with 6 stages

C_o: Capacity of a charging ceramic capacitor in each module

C_1: Stray capacity between 2nd through 5th module and the container wall in each stage

C_2, C_3: Stray capacity between the first and the last (6) stage module, including end effect

C_g: Capacity of a spark gap in each stage

The values such as R, R_g, L, L_e, L_0, C_1, C_2, C_3, and C_g are uncontrolled parameters which are specific to the design of CMG i.e. the element configulation and its layout, and their materials used. On the other hand, R_0 and C_0 are only controlled parameters which play an important role to obtain the desired impulse waveform.

In general, the circuit equations with n stages are expressed as follows[2];

$$L\frac{dI_1}{dt} + \frac{1}{C_o}\int I_1 dt + RI_1 + \frac{1}{C_g}\int (I_1 - i_1)dt + \frac{1}{C_2}\int (I_1 - I_2)dt = 0$$

$$L\frac{dI_2}{dt} + \frac{1}{C_0}\int I_2 dt + RI_2 + \frac{1}{C_a}\int (I_2 - i_2)dt + \frac{1}{C_1}\int (I_2 - I_3)dt$$

$$+ \frac{1}{C_2}\int (I_2 - I_1)dt = 0$$

$$L_a\frac{dI_n}{dt} + \frac{1}{C_0}\int I_n dt + RI_n + \frac{1}{C_a}\int (I_n - i_n)dt + \frac{1}{C_1}\int (I_n - I_{n-1})dt$$

$$+ \frac{1}{C_3}\int (I_n - I_{n+1})dt = 0$$

$$\frac{1}{C_3}\int (I_{n+1} - I_n)dt + L_a\frac{dI_{n+1}}{dt} + R_a I_{n+1} = 0$$

$$L_a\frac{di_1}{dt} + R_a i_1 = \frac{1}{C_a}\int (I_1 - i_1)dt$$

$$L_a\frac{di_n}{dt} + R_a i_n = \frac{1}{C_a}\int (I_n - i_n)dt \qquad (1)$$

The waveform analysis was carried out to solve these equations at an initial condition, giving C_0, C_1, C_2 and C_3 , charged to an initial voltage, V. A Runge-Kutta-Gill's method was applied to solve the equations.

5 Results of calculation

Waveform analysis result of CMG is shown in Fig.6 (1) through (8). The calculation was made on the basis of the following element values*; R= 2.20 ohms, R_0= 26.0 ohms, R_g= 0.10 ohms, L= 26 NH, L_1= 10 NH, L_2= 98 NH, L_0= 4654 pH, C_0= 4700 pH, C_1= 81 pF, C_2= 88 pF, C_3= 108 pF, and C_4= 10 pF.

The output impulse voltage waveform is shown in Fig.6 (1) with changing R_0 as a parameter. The peak value increases as R_0 increases. The rise time and tail time, however, become longer and the pulse duration reduces its half peak value as R_0 increases. Namely, the increase of R_0 is effective to raise the pulse height and not desirable to obtain a quasi rectangular wave.

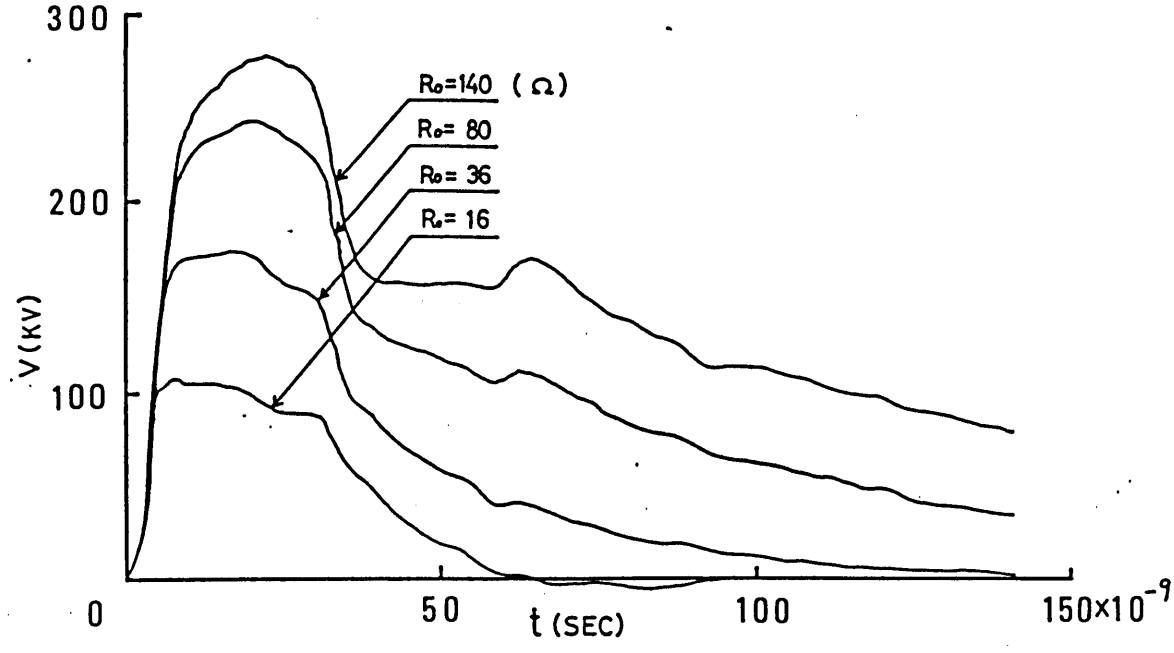

Fig. 6 Waveform analysis of CMG

(1) R_θ dependence

The output impulse voltage waveforms are shown in Fig.6 (2) with changing the inductance L, existed in a module as a parameter. The rise time and pulse height increase as L decreases, however, the pulse duration becomes shorter. Namely, the increase of L is effective to obtain a quasi rectangular wave with decreasing the pulse height.

With changing the inductance L_e of the last stage module, the output impulse voltage waveforms are shown in Fig.6 (3). This last stage module is connected to the output resistance so that the configulation of the last module is slightly different from others. Therefore, the influence of the inductance L_e is considered to slightly differ from L_e in the other module. The decrease of L_e makes the rise time shorter and also increases the pulse duration.

The above results show that to obtain a quasi rectangular wave, the inductance of the last stage module should be reduced as possible as could, namely, the conpact design with a short length is required.

The output impulse voltage waveforms are shown in Fig.6 (4) with changing R, the internal resistance of a charging capacitor plus a resistance in the circuit per unit module as a parameter. The decrease of R enables the pulse height to increase and causes harmonics which are

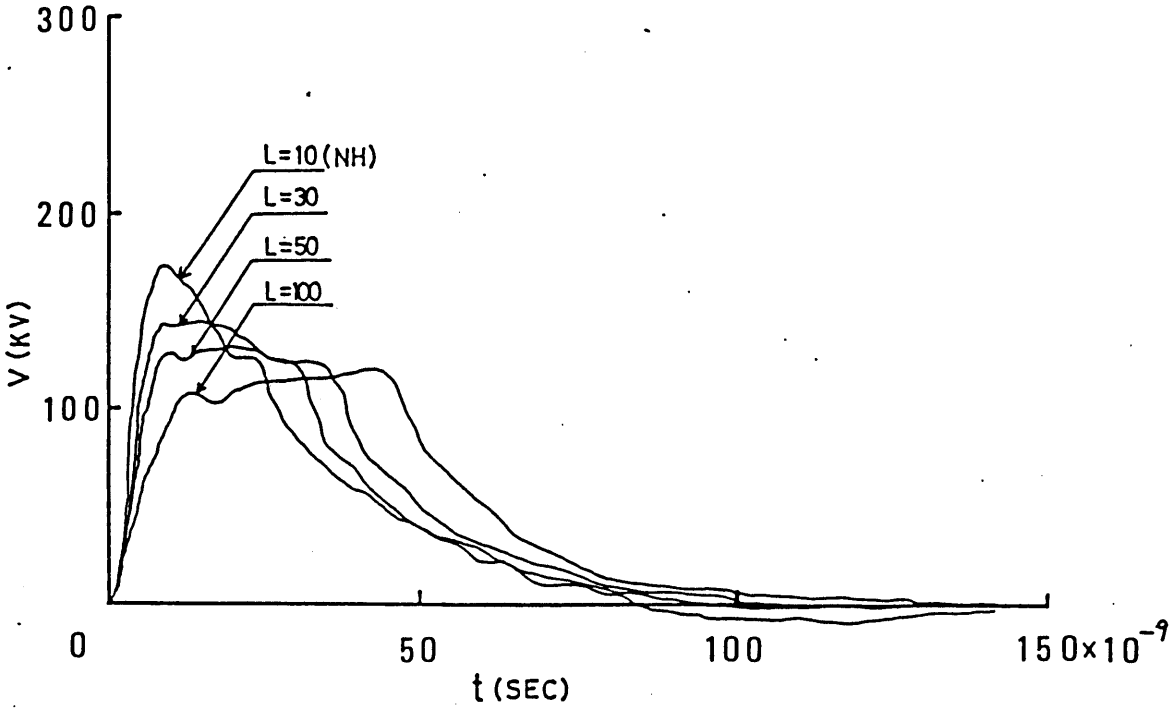

Fig. 6 Waveform analysis of CMG

(2) L dependence

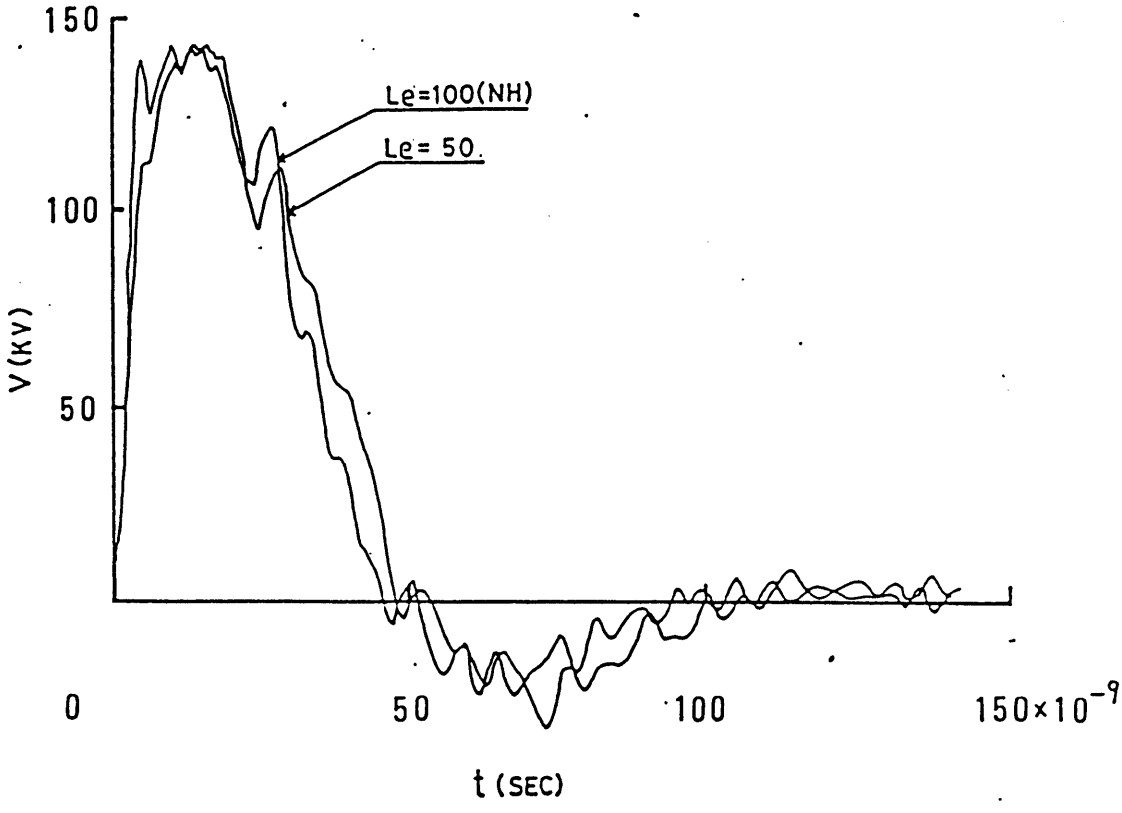

Fig. 6 Waveform analysis of CMG

(3) L_e dependence

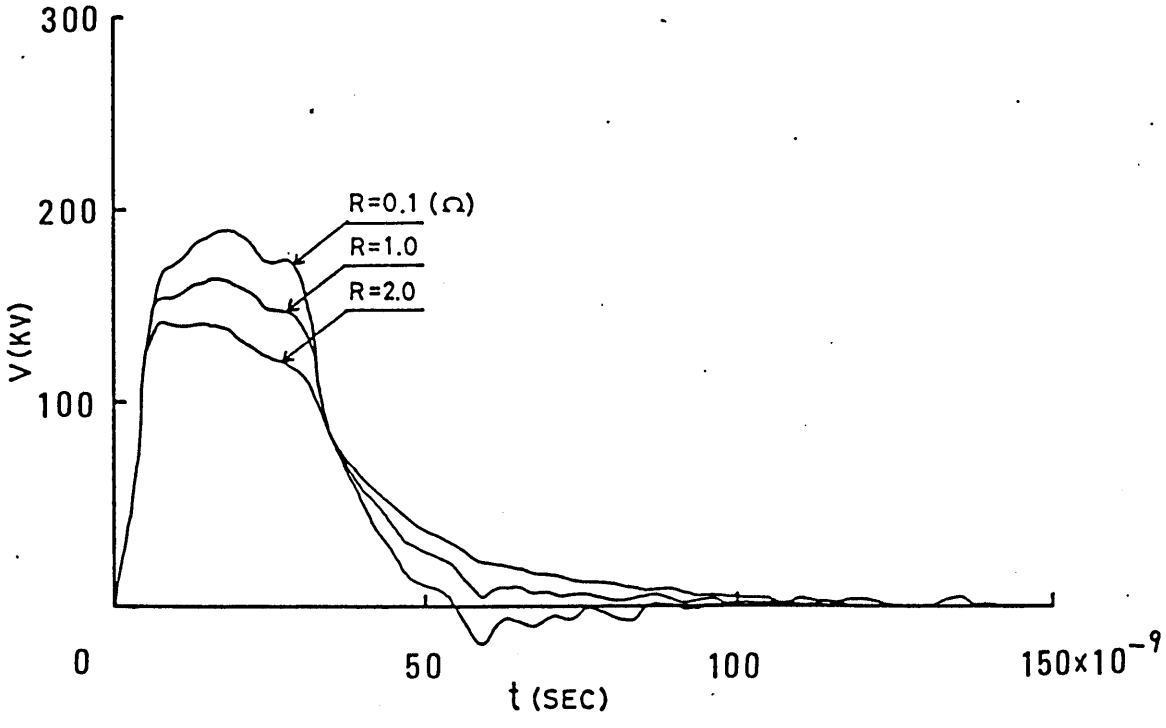

Fig. 6 Waveform analysis of CMG

(4) R dependence

negligible. In design, it is necessary to decrease the internal resistance.

With changing C_0, capacity of a charging capacitor in each module as a parameter, the output impulse voltage waveforms are shown in Fig.6 (5). The increase of C_0 has no influence on the rise time, and makes the pulse height and pulse duration larger. Namely, the capacity has nothing to do with the rise time and plays an important role to form the wave tail. In design, the capacity to comply with the pulse duration to be applied should be selected.

The output impulse voltage waveforms are shown in Fig.6 (6) with changing C_1 , stray capacity between 2nd through 5th module and container wall (capacity of the insulating oil) as a parameter. The decrease of C_1 makes the rise time shorter and causes harmonics in the wave. In design, the rise time and pulse duration which we need should be considered.

The output impulse voltage waveforms are shown in Fig.6 (7) with the values of C_a ,20 pF and 50 pF. The waveform of C_a ,50 pF, is represented to be superimposed on the waveform of C_a ,20 pF with harmonics. It is desirable to decrease the value of C_a to reduce

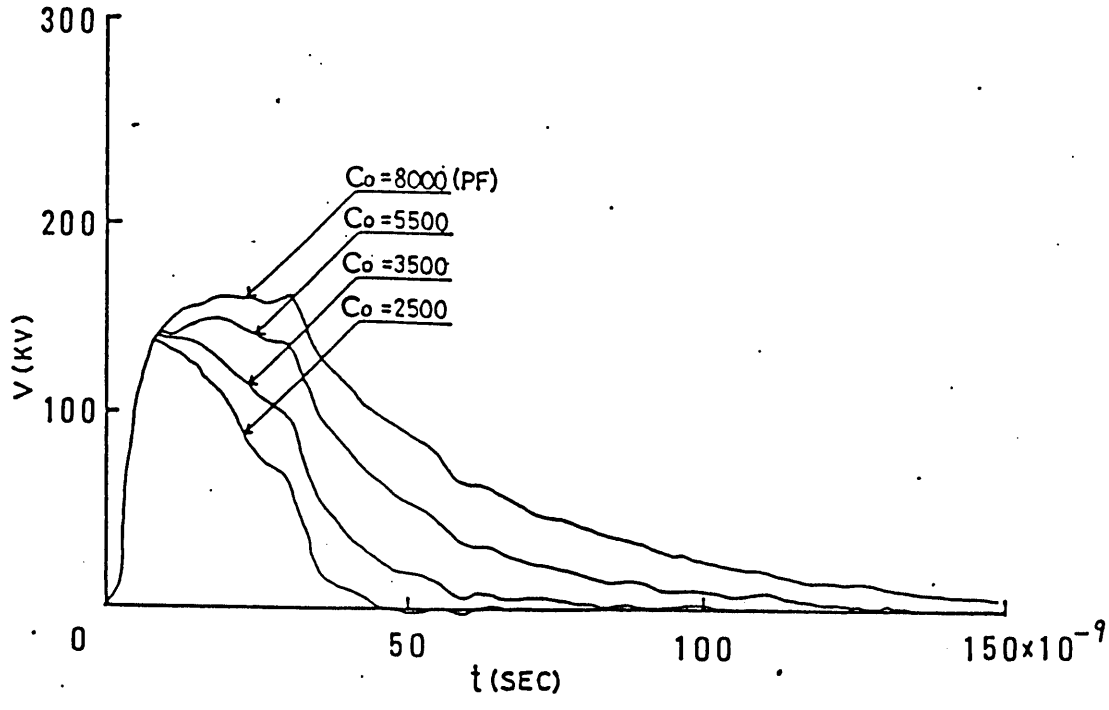

Fig. 6 Waveform analysis of CMG

(5) C_0 dependence

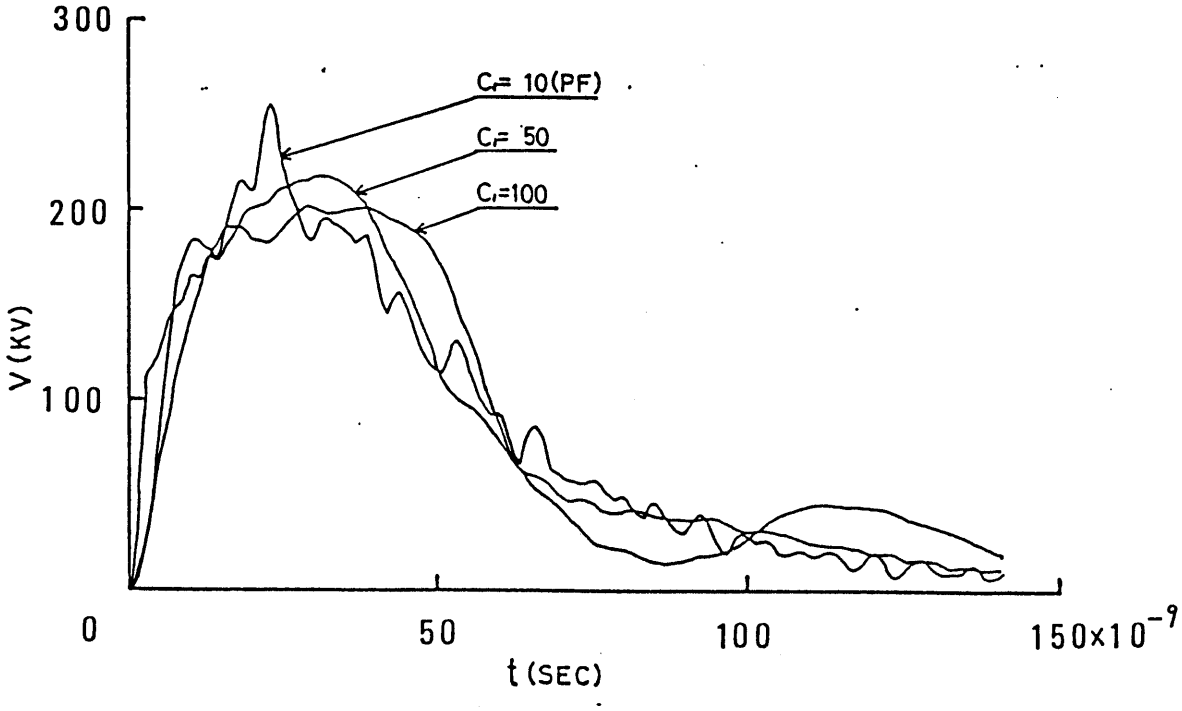

Fig. 6 Waveform analysis of CMG

(6) C_t dependence

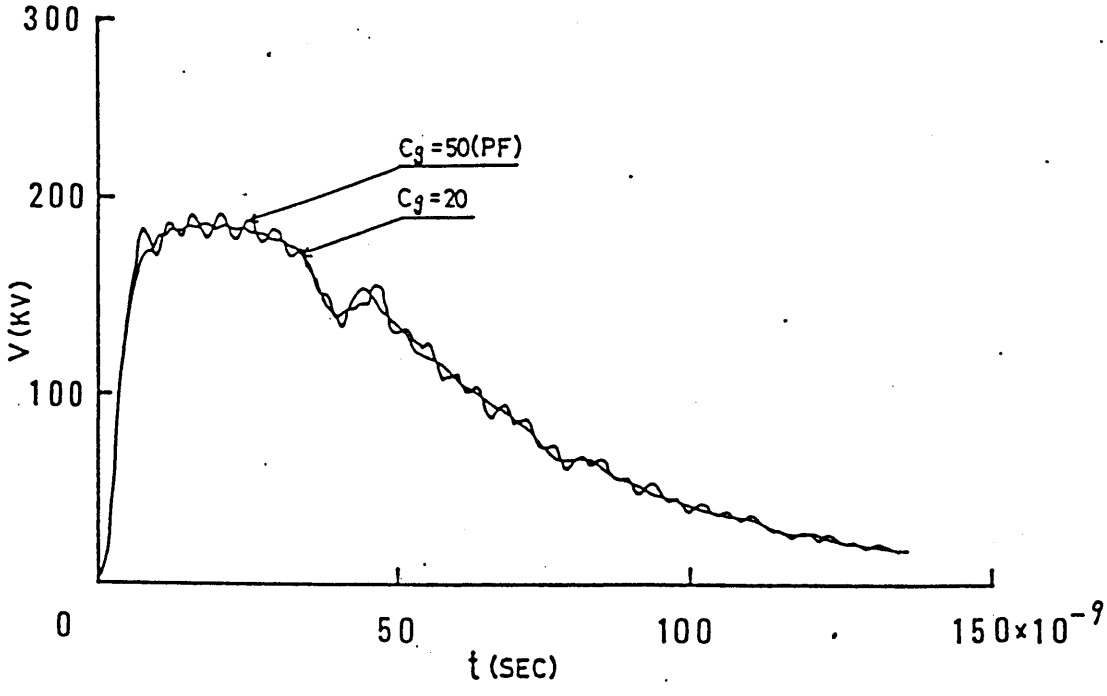

Fig. 6 Waveform analysis of CMG

(7) C_a dependence

the harmonics. The value of C_g depends on gap configulation and the kind of gas filled in the gap.

The output impulse voltage waveforms are shown in Fig.6 (8) with changing a number of modules as a parameter, in keeping the value of each element constant. The increase of a number of modules reduces the harmonics and makes the rise time shorter,however, the pulse duration becomes shorter and its waveform approaches to a trianlge.

6 Improvement of waveform

In the previous section, the output impulse voltage waveforms are examined. The design of ns quasi rectangular pulse may be investigated in this section.

6.1 Improvement of rise time

In order to make the rise time shorter, L and L_g must be reduced. Too much reduction for them causes the quasi rectangular pulse to be

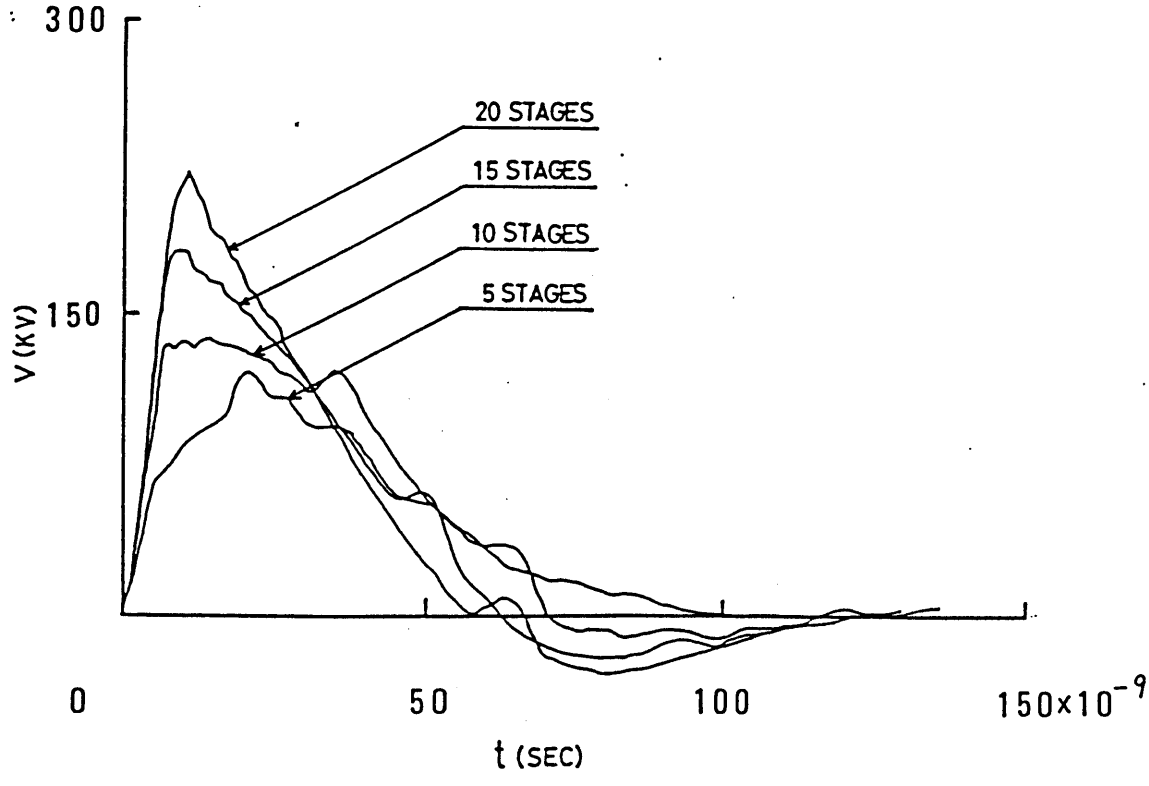

Fig. 6 Waveform analysis of CMG

(8) Number of module dependence

distorted. These values should be carefully examined at an initial stage of the design.

6.2 Reduction of pulse duration

In order to reduce the pulse duration, C_o should be decreased and C_1 should be increased. It is not possible to change C_1 because that value depends on the configulation of the module and a permittivity of the medium filled inside the module and the container wall. Therefore the best way for that is to decrease the C_θ. If C_θ is decreased in each stage, the equivalent series resistance may be increased and its efficiency is to be decreased. Moreover, the reduction of trigger effect caused by the decrease of C_θ get worthen the rise characteristics. To avoid these situation , the reduction of the equivalent series resistance ,by decreasing the capacity in only the last stage enables the pulse duration to be obtained without decreasing the efficiency and the trigger characteristics.

6.3 Reduction of harmonics

C_a , C_1 , and L_a are the most concerned in harmonics of the waveforms. These elements are considered to be existed in the module so that it is necessary for these elements to be reduced as possible as could in design stage.

7. Investigation of output impulse voltage waveforms

The calculated and measured waveforms will be examined in this section. Typical two representative waveforms are shown in Figs. 7 and 8. Fig. 7 shows the measured and calculated waveforms in the case of CMG with 6 stages (where C_0 = 4700 pF employed). The waveform with rise time of 10.8 ns and pulse duration at half peak of 30 ns is observed in the oscilloscope screen and the waveform with rise times of 11 ns and pulse duration at half peak of 32 ns is obtained in the calculation. A good agreement between both waveforms is observed.

Fig. 8 shows the measured and calculated waveforms in the case of

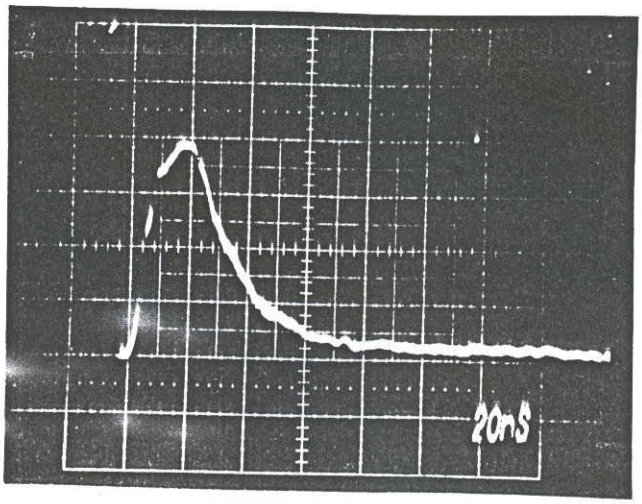

(a)

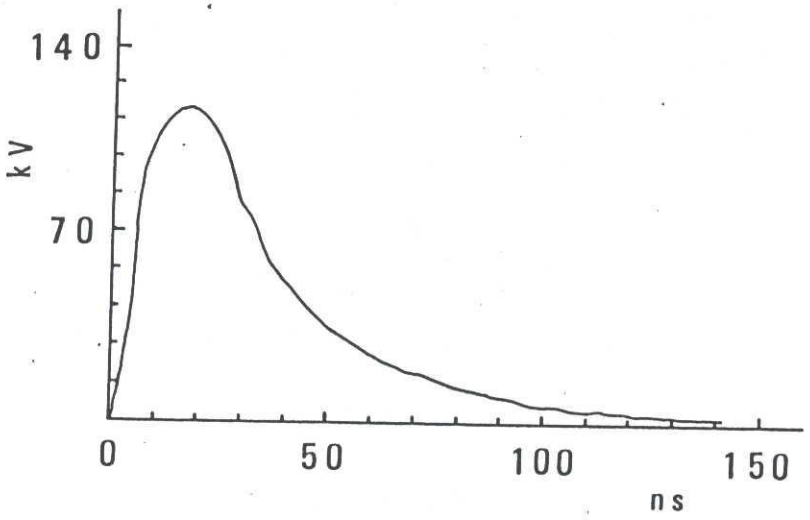

(b)

Fig. 7 Measured and calculated waveforms for CMG

(a) a waveform observed in an oscilloscope

applied voltage: 114 kV, sweep: 20 ns

(b) calculated waveform by a computer

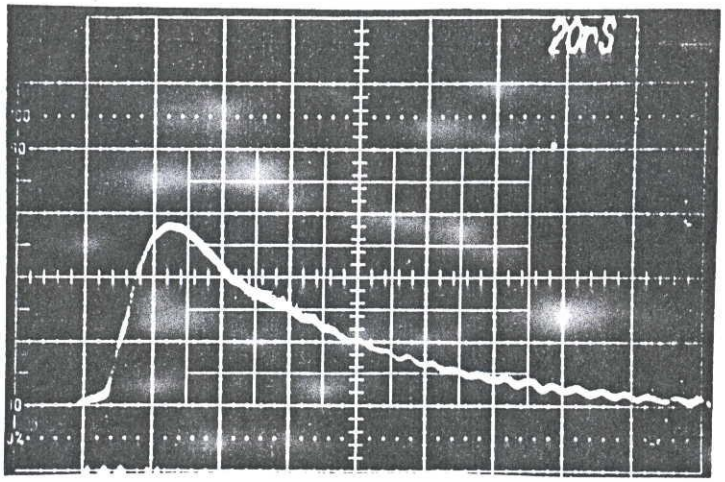

(a)

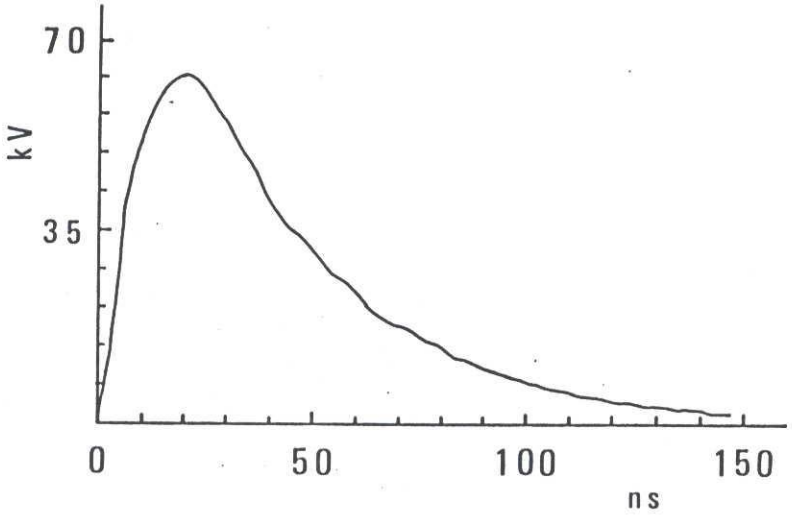

(b)

Fig. 8 Measured and calculated waveforms for CMG

(a) a waveform observed in an oscilloscope

applied voltage: 63 kV, sweep: 20 ns

(b) calculated waveform by a computer

CMG with 4 stages (where C_0 = 5000 pF employed). The waveform with rise times of 14.8 ns and pulse duration at half peak of 54 ns is observed in the oscilloscope screen and the waveform with rise times of 14.5 ns and pulse duration at half peak of 55 ns is obtained in the calculation. A good agreement between both waveforms is also observed.

As stated above, the computer-aided design for CMG can enable the author to simulate the impulse waveform and is helpful to design a desired waveform.

8 Measurement of ns current pulse

The schematic diagrams for measuring currents and its equivalent circuit are shown in Fig. 9 and 10. If $R \gg \omega L$, $t \ll RC$, the following relation can be obtained,

$$Vc(t) = \frac{1}{C}\int i\,dt = \frac{\Phi(t)}{RC} \qquad (2)$$

where ω is the maximum angular frequency for Φ,

t is time

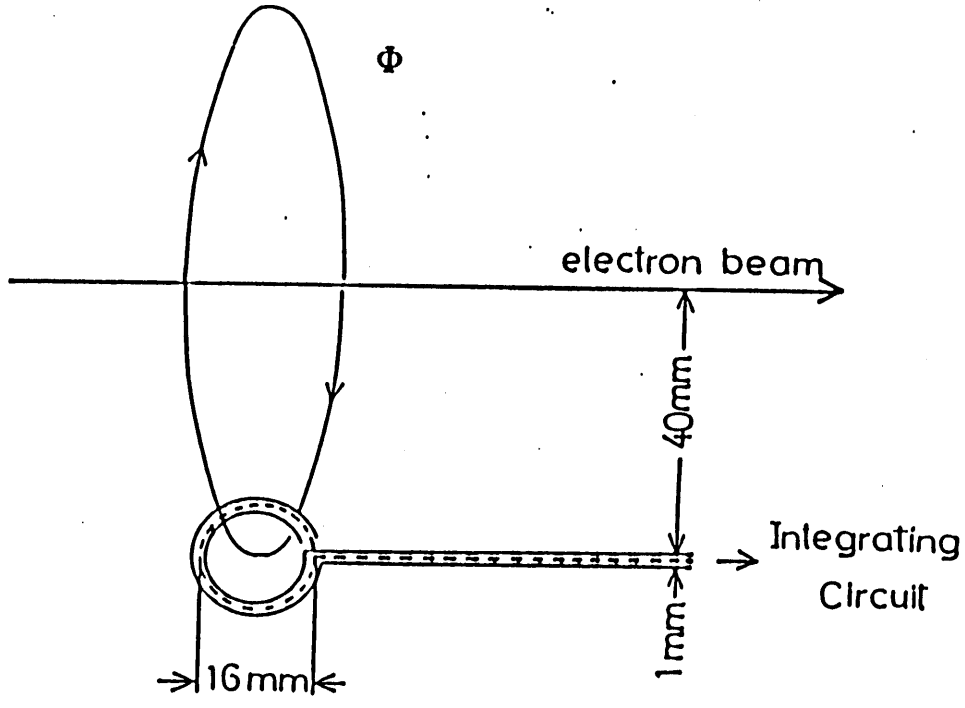

Fig. 9 Configuration arrangement of pick-up coil

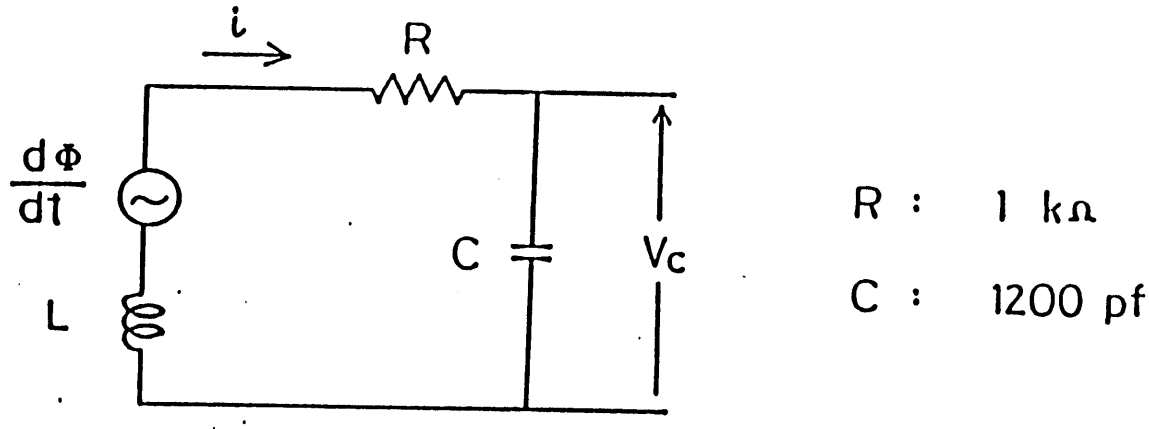

Fig. 10 The equivalent circuit of pick-up coil

Induced magnetic flux is

$$\Phi(t) = KnI(t) \tag{3}$$

where K is a constant decided by geometrical arrangement of the coil and its current distribution, and n is a number of coil turns.

Measured current I(t) is

$$I(t) = \frac{RC\ell}{\mu_0 nA} \cdot Vc(t) \tag{4}$$

where μ_0 is a permeability of the space for current measurement,

A is cross section, ℓ is a average length of solenoid

From (2) through (4),

$$K = \frac{\mu_0 A}{\ell}$$

8.1 Observation of ns current pulse

The current measurement of ns electron beam was carried out by pick-up coil with the use of CMG.

The response characteristics of ns rectangular current pulse of the measurement circuit and its current vs. voltage characteristics are shown in Fig.11 and 12, respectively. There is no distortion between the osilloscope voltage and a measured voltage and a linear characteristics were observed between them. From these results, k may be obtained.

K=1200 , calculated from Fig.9

K=1430 , measured from Fig.12

The calculated values and measured values show very close values to each other.

Fig.13 shows the voltage waveform of ns electron beam and the current waveform. The good similarity has been observed each other.

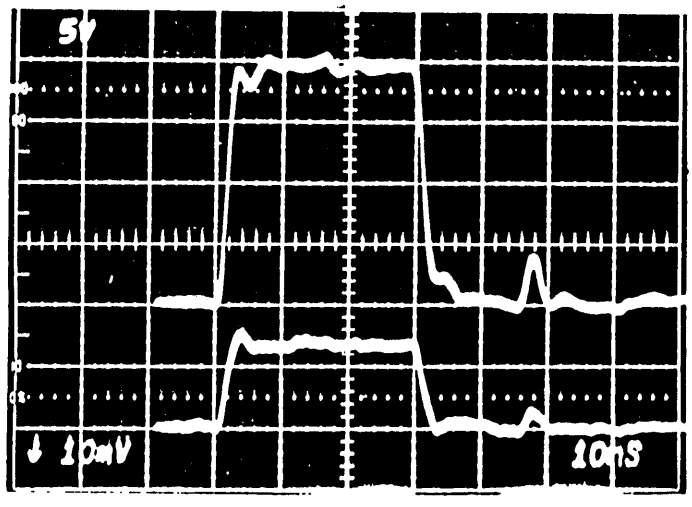

Fig. 11 Response of pick-up coil by test pulse

Upper trace: test pulse,5 A/div.,10 ns/div.

Lower trace: coil voltage,10 mv/div.,10 ns/div.

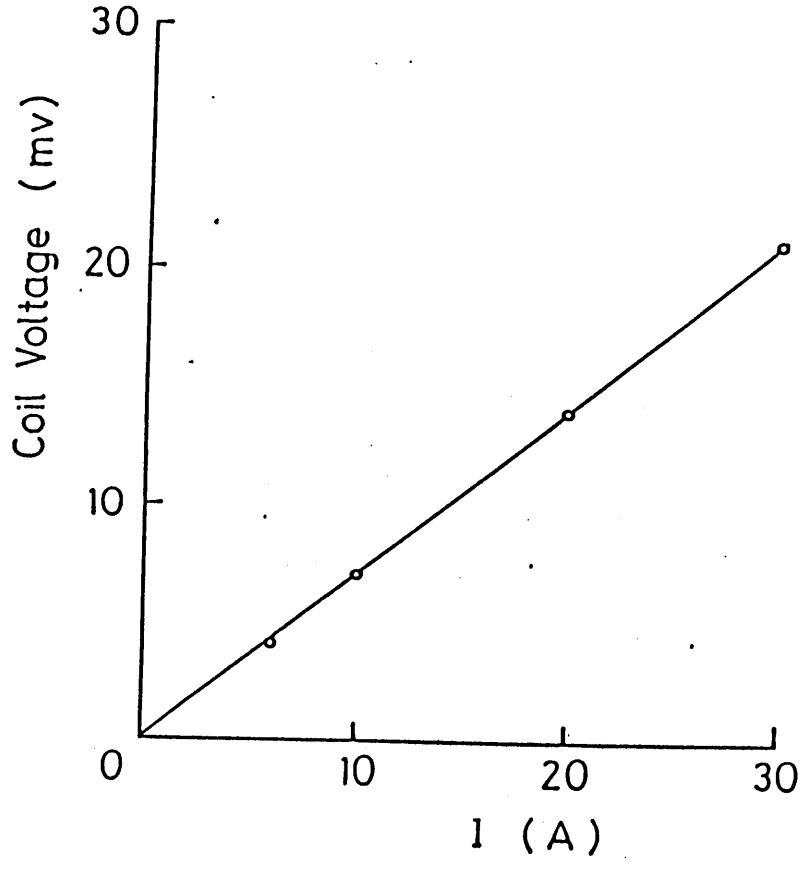

Fig. 12 Voltage vs. current characteristics of pick-up coil

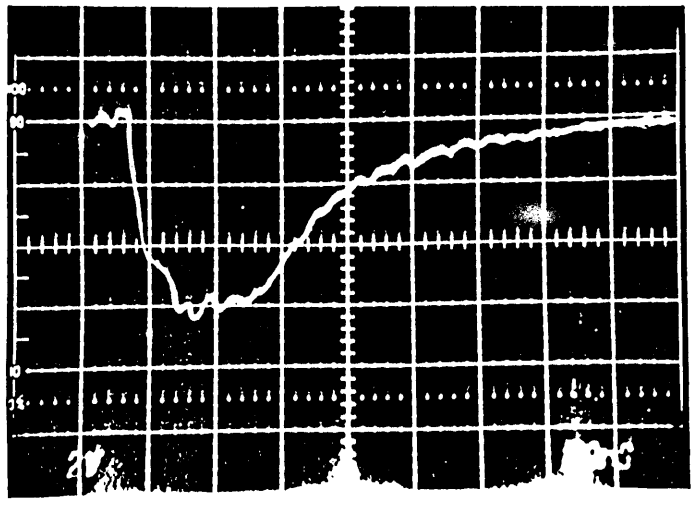

(a)

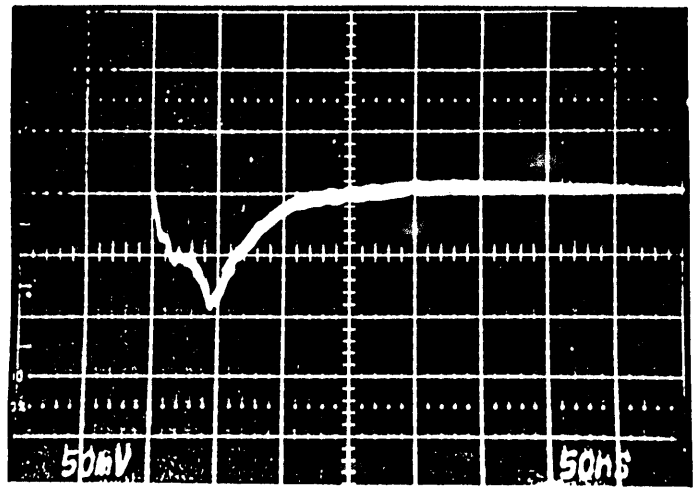

(b)

Fig. 13 Voltage and current oscillograms of ns beam

(a) Diode voltage: 60 KV/div.,20 ns/div.

(b) Electron beam current: 100 A/div., 50 ns/div.

9 Conclusions

The author has developed ns impulse voltage generator to obtain the impulse voltage with a sharp rise time and a short pulse duration. The following describes salient conclusions:

(1) The output impulse voltage of the CMG can be analyzed by the distributed constant circuits, whose each stage forms a module.

(2) The reduction of L and L_s is required to increase the rise time of the impulse voltage.

(3) The reduction of L and C_0 is required to obtain the impulse voltage with a short pulse duration. The reduction of C_0 is the most appropriate because it is difficult to change the value of L, which is internally existed in the module.

(4) The values of C_d, C_1, and L_e should be as small as possible to reduce the harmonics in the impulse voltage.

(5) Current measurement can be made by the pick-up coil with a single turn.

References

1. Y. Kubota, S. Kawasaki, A. Miyahara and H.M. Saad,
Coaxial Marx generator for producing intense relativistic electron beams,
Jpn. J. Appl. Phys. 13, pp.260-263 (1974)

2. Y. Kubota, J. Kodaira, and A. Miyahara
Study of the rectangular-like output waveforms of a 720 kV coaxial Marx generator
Jpn. J. Appl. Phys. 20, pp.2397-2400(1981)

3. Y. Sakato, T. Hashimoto, M. Obata and T. Fuzioka,
Low-impedance, coaxial-type Marx generator with a quasi-rectangular output waveform,
2nd IEEE international pulsed power conference digest of papers
Lubbock, TX, USA, pp.165-171 June 1979

4. H. Matsuzawa and T. Akita,
Output voltage waveform improvement of the coaxial Marx-type high-voltage generator,
Rev. Sci. Instrum. 56(12), pp.2287-2289 (1985)

5. Yukimitsu Kawada, Sumikazu Shamoto and Tatsuzo Hosokawa,
Nanosecond-pulse breakdown of gas-insulated gaps,
J. Appl. Phys. 63,, pp.1877-1881 (1988)

6. Yukimitsu Kawadá and Tatsuzo Hosokawa,
Breakdown phenomena of gas-insulated gaps with nanosecond pulses,
J. Appl. Phys. 65, pp.51-56 (1989)

7. Yukimitsu Kawada and Tatsuzo Hosokawa,
Observation of nanosecond-pulse breakdown of gas-insulated gaps by image converter camera
J. Appl. Phys. accepted for publication and to be published in 15 January 1990 issue of the J. Appl.Phys.

8. Hiroo Obara,

Waveform analysis for Marx generator,

B.Sc. Thesis, Nagoya institute of Technology, (1981)

Chapter II Nanosecond Pulse Breakdown of Gas-Insulated Gaps*

1 Introduction

Many research works on breakdown mechanism of gaseous discharge have been carried out. In the regime where $p\ell$ (p : pressure, ℓ : gap length) and overvoltage ratio are low, Townsend's theory may be applicable. Streamer theory by Loeb, Meek and Raether is dominant in the regime of high $p\ell$ and high overvoltage ratio.[1],[2],[3] Although electron emission from the cathode is, of course, required to establish flashover, the main difference from Townsend's theory generation mechanism is that a discharge can develop regardless of γ (electron emission from cathode by secondary mechanism) at the beginning of breakdown dominated by applied static field. This is an essential difference between

* Publication in the 15 March 1988 issue of the Journal of Applied Physics { J. Appl. Phys. 63, 1877 (1988) }

Townsend's theory and streamer theory. The regime of validity of these models, however, is not clear because of their complexity.

On the other hand, it is generally understood that impulse voltage breakdown shows different properties depending on rise time and pulse duration. This is due to the fact that transition process from an electron avalanche to a streamer and its development are influenced by the applied field and duration. The drift velocity of the electrons, the space charge field ahead of an electron avalanche, and the residual positive ion group seem to be strongly involved with the transition.

Breakdown phenomena of gas-insulated gaps, obtained with nanosecond pulse, have already been reported by Kunhardt and Byszewski [4] and they have explained the development of a streamer by a runaway electron model.

In the transition process from an electron avalanche to a streamer, cosidering mutual actions by space charge field due to a group of electrons ahead of electron avalanche and applied field of the gap, the author agrees with the physical possibility of such electrons. Namely, one electron emitted from the cathode develops into a gap in forming the avalanche. The electrons produced by ionization of collisions are located ahead of the eleotron avalanche. The movement

of the positive ions is short in comparison with the drift velocity of electrons so that the positive ions are considered to stand still where they are produced.

Therefore, only positive ions stand in line along the avalanche path and, moreover, the maximum density of positive ions occurs next to the group of electrons ahead of the avalanche. The electrons are retarded by these ion groups. This retarding force strongly increases with development of the avalanche. The electrons actually stop advancin at a certain distance. At this stage, the electrons are more strongly attracted by positive ions and conversion into plasma with high conductivity occurs. In this transition process from an avalanche to a streamer, runaway electrons are considered to the electrons escaped from the electron avalanche. The run away is generated by a repulsive force due to the electrons themselves and the applied field and the developing streamer by chain reactions of these electrons. Theoretical and experimental approaches have been carried out by many researchers to investigate the runaway electrons. [4],[5],[6] These articles, however, do not mention about $p\ell$ vs. flashover characteristics of the gaseous discharge. For the purpose of clarifying the streamer formation and its development, an investigation of $p\ell$ vs. flashover characteristics, using impulse voltages with short duration, is

considerd to be very important.

The author has carried out research on breakdown phenomena in several kinds of gases, that were subjected to impulse voltages (10.8 × 30 ns). The impulse voltages have an influence on the time of streamer formation and allowed investigating the transition from an electron avalanche to a streamer in addition to the flashover mechanism of gas-insulated gaps. As a result of our investigation, I found that the 50% probability of flashover voltage and the property of luminosity of the gas depends on the kind of gases such as air, N_2, and O_2. These properties also differ for different pulse durations.

This research paper is the first issue in a series of articles and will describe mainly experimental results such as the 50% probability of flashover voltage of gas-insulated gaps in air, N_2, and O_2, and the properties of luminosity obtained by still camera photographes.

Moreover, this paper indicates that the flashover voltage depends on pulse duration of the impulse voltage. The author also attempted to investigate the streamer formation process on the basis of $p\ell$ vs. flashover phenomena.

The observation of the luminosity in the gap obtained by an

Image Converter Camera, is scheduled to be reported in a second article that will address time lag from voltage application to flashover.

2 Apparatus

The diagram of this experiment is shown in Fig. (1). A high voltage impulse generator used in this study is a co-axial type Marx generator.[7-10] The maximum output voltage can reach 130 kV by changing the charging voltage of the Marx generator and the output resistance ($CuSO_4$ solution). Uniform test gaps are stailess steel Rogowski electrodes with a diameter of 9 cm. The stainless container in which the test gaps are located was evacuated to 10^{-5} torr with the use of a rotary pump and a diffusion pump and then various gases such as air, N_2, and O_2 are backfilled into the container to the desired pressure. To minimize the fluctuations of flashover voltage, ultra-violet rays continuosly illuminate the surface of the cathode. Each shot was made at one-minute intervals to allow stabilization from the aftereffect of the previous flashover.

A waveform of the impulse voltage was recorded by a Tektronix

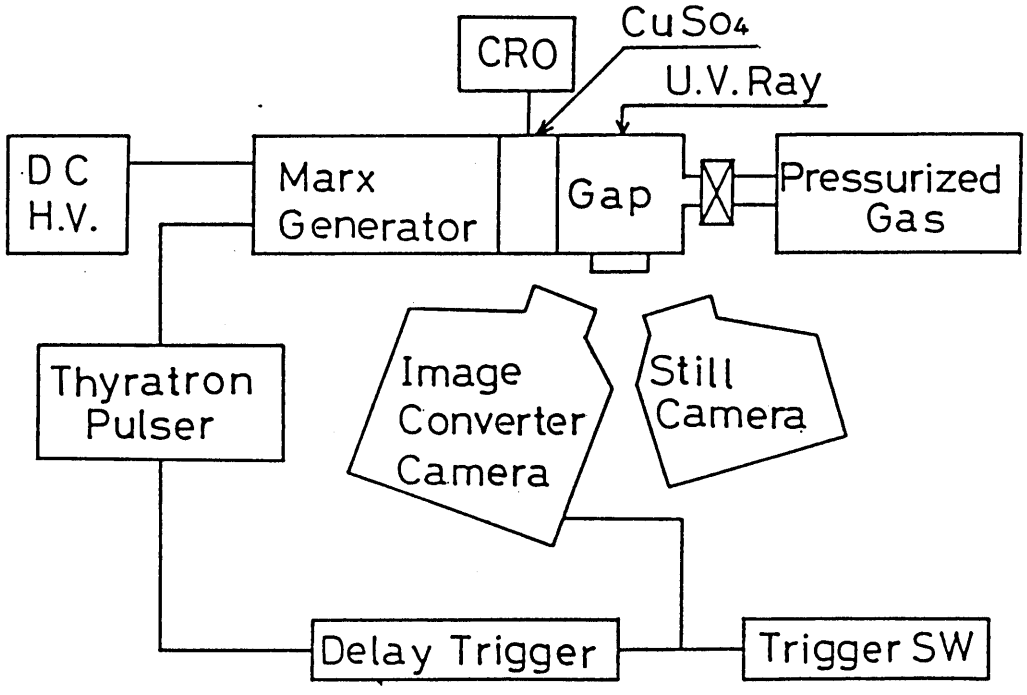

Fig. 1 Experimental circuit arrangement

storage oscilloscope (7834) using the $CuSO_4$ solution as a resistance divider. An impulse waveform observed during this test is shown in Fig. (2). A rise time of 10.8 ns and pulse duration at half peak of 30 ns are obtained.

3 Experimental Results

The author will now describe the breakdown properties of various gases such as air, N_2, and O_2 in uniform fields, subjected to impulse voltages from the coaxial Marx-type impulse generator. The breakdown properties reported in this article were obtained using gap conditions of ℓ = 1, 2 and 3 cm and pressure between 330 and 1520 torr.

Figures (3) to (8) show the breakdown characteristics of various gases. V_{50} is the 50% probability of flashover voltage (called 50% flashover voltage hereafter) and is obtained by an interpolation method. In general, breakdown of a gas may be caused by the ionization from the collision of electrons. The magnitude of the electron energy obtained from the field is the main factor causing the breakdown. In this paper, flashover characteristics are reported using the

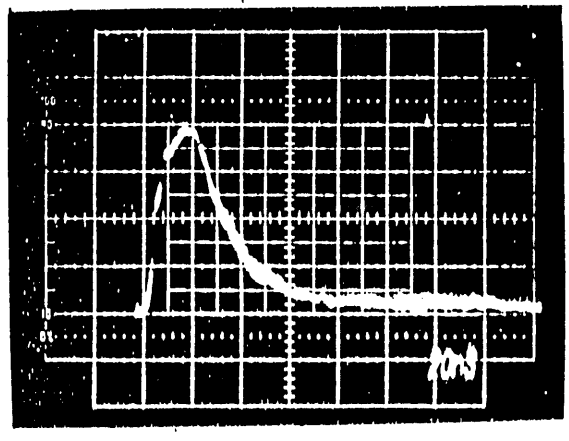

Applied voltage: V

114 kV

Sweep: 20 ns

Fig. 2 Impulse waveform

parameter $p\ell$, which represents the energy an electron obtains in a mean free path in a gas.

Fig. (3) shows the breakdown characteristics of air. In this figure, V_s indicates static breakdown voltage of the gap. When applying an impulse voltage, the author needed a higher voltage than V_s to cause flashover of the gap. When applying higher voltages than V_s to the gap, two different states of luminosity were observed in the gap. Namely, as the applied voltage increases, broad luminosity, as shown in Fig. (4), was observed in the whole gap at the beginning. The intensity of the luminosity increases with increasing applied voltage. At yet higher voltages, the intensity of the luminosity increases and, as shown in Fig. (5), blue-white filamentary luminosity started to be observed on both cathode and anode surfaces. The filamentary luminosity was connected with broad luminosity in the middle of the gap. In this state of breakdown, an abrupt decrease of the applied voltage cannot be observed so that flashover does not occur at this stage. Further increase of the applied voltage causes more intensive-filamentary luminosity that bridges the gap and an abrupt decrease of the voltage was observed on the oscilloscope screen. As described above during the breakdown of air, the following breakdown property was observed; i.e., broad luminosity appears at the beginning and then filamentary

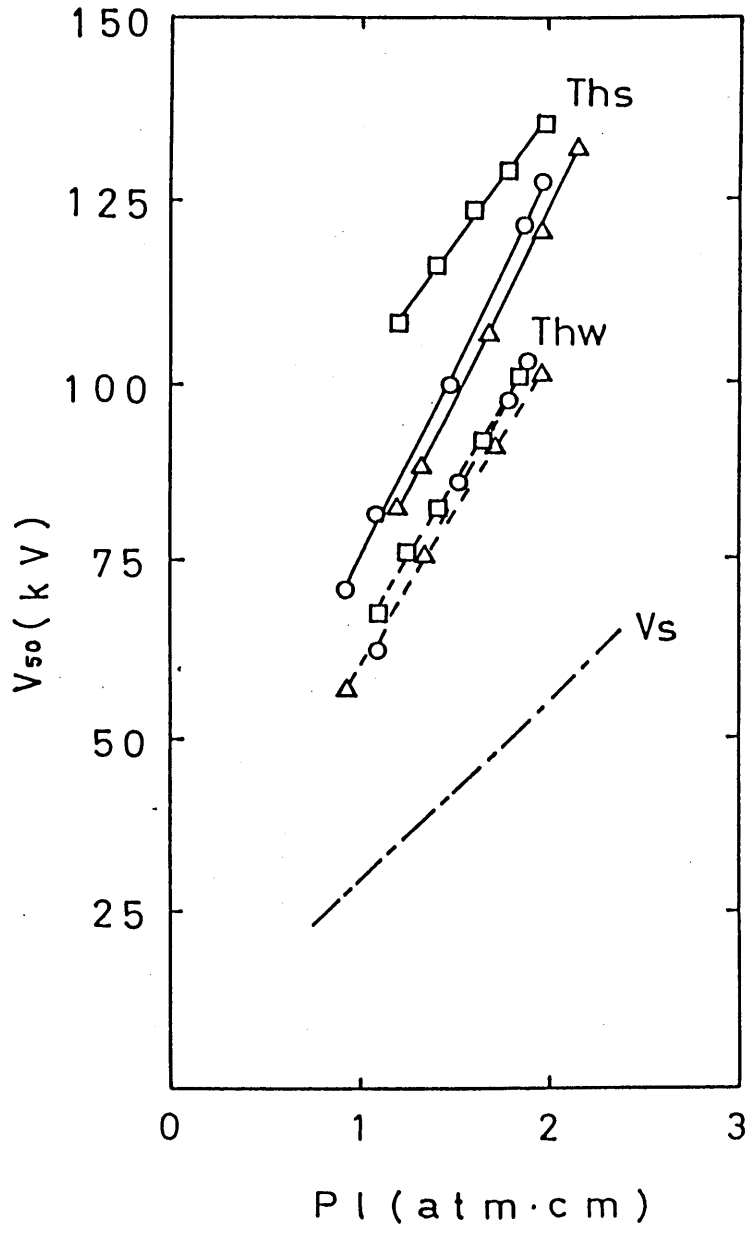

Fig. 3 50% flashover voltage vs pℓ characteristics of air

□ : ℓ = 3 cm, △ : ℓ = 2 cm, ○ : ℓ = 1 cm

Ths: Impulse waveform (10.8×30 ns)

Thw: Impulse waveform (10.8×74 ns)

V_s : Static breakdown voltage

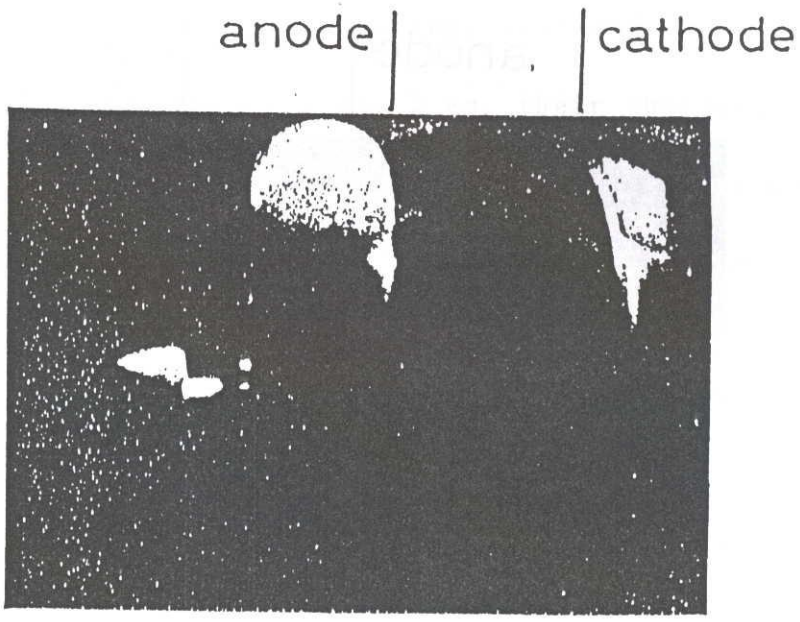

Fig. 4 Photographic evidence (state of broad luminosity)

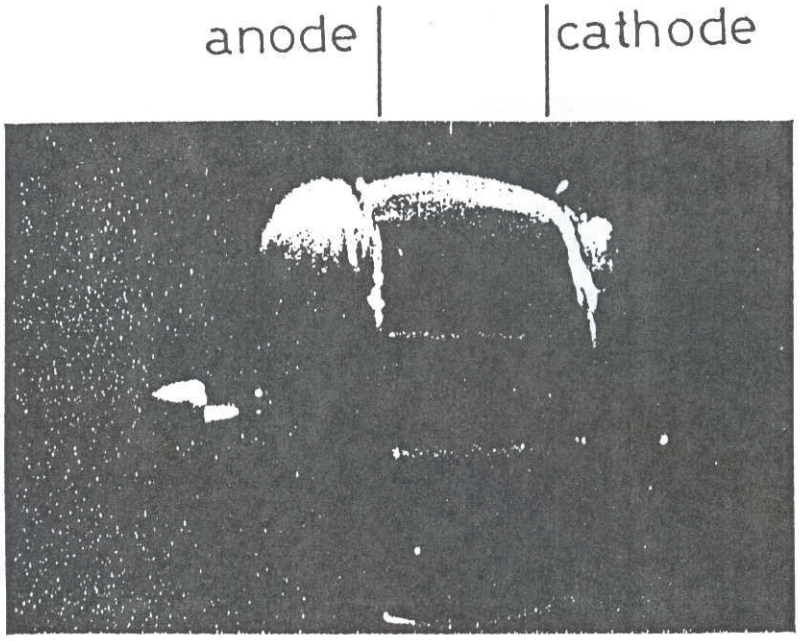

pl : 1.5 atm·cm
l : 3 cm
V : 120 kV

Fig. 5 Photographic evidence (state of filamentary luminosity)

luminosity is caused, developing into flashover of the gap.

Fig. (3) shows the relation between $p\ell$ and the 50% flashover voltage in final breakdown, i.e., flashover using two different pulse durations, 30 ns and 74 ns (the waveforms of which are hereafter called Ths and Thw, respectively). As $p\ell$ increases, the 50% flashover voltage linearly increases. The voltage, however, showed different values that varied with gap length. At ℓ = 1 and 2 cm, their characteristics are quite similar and the 50% flashover voltage seems to be the same within their fluctuations. At ℓ = 3 cm, the situation is different from the others and the 50% flashover voltage is 10 to 15 kV higher at the same $p\ell$.

On the other hand, in the case of an impulse voltage with longer duration (74 ns), the appearance of luminosity was similar to those of shorter impulse voltage (10.8 × 30 ns). More frequently observed is the appearance of filamentary luminosity leading to channel breakdown at about 15 kV lower than impulse voltage with Ths.

Fig. (6) shows the breakdown characteristics of N_2. The state of luminosity observed in the gap showed similar properties to that of air. Broad luminosity appears in the gap as the impulse voltage increases and at higher impulse voltages, filamentary luminosity develops into flashover of the gap. In the breakdown of N_2, the 50%

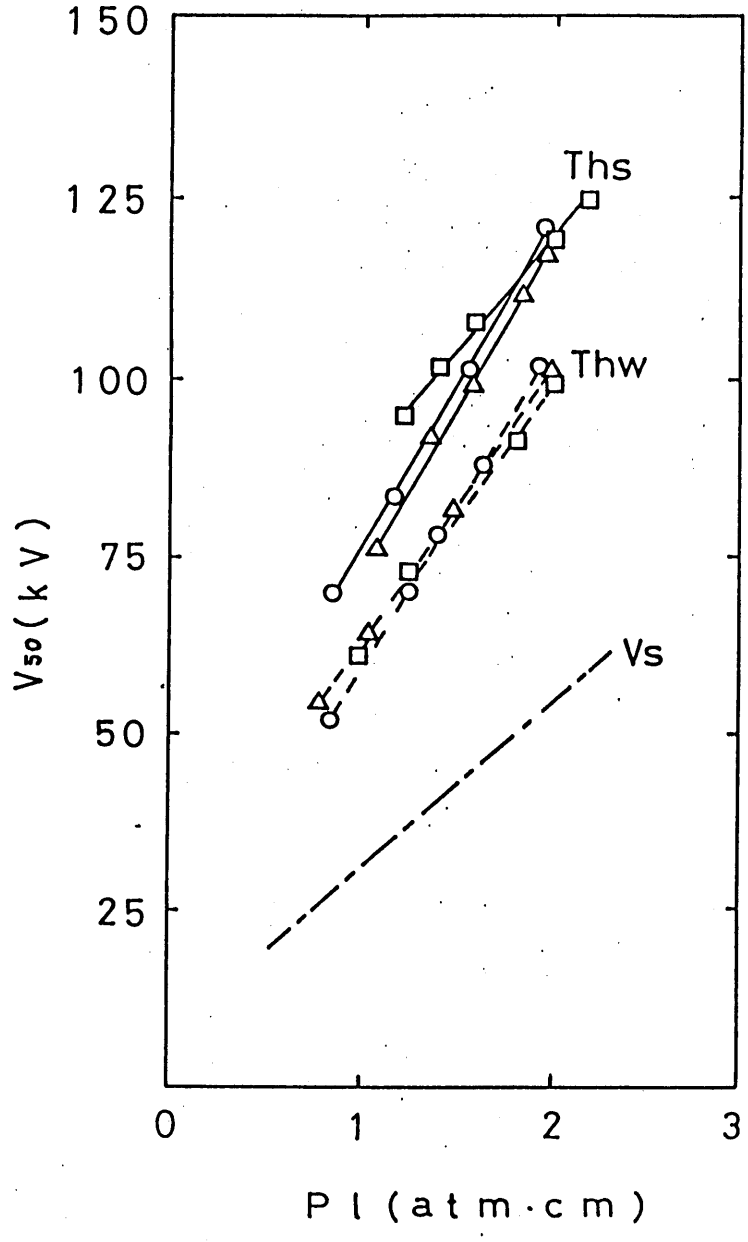

Fig. 6 50% flashover voltage vs pℓ characteristics of N_2

□ : ℓ = 3 cm, △ : ℓ = 2 cm, ○ : ℓ = 1 cm

Ths: Impulse waveform (10.8×30 ns)

Thw: Impulse waveform (10.8×74 ns)

V_s : Static breakdown voltage

flashover voltage also showed very close values at ℓ =1 and 2 cm. At ℓ =3 cm, the difference of the flashover voltage due to the gap length was not observed at the region of 2 atm-cm. Distinctive differences, however, were observed at lower pℓ than 2 atm-cm. The 50% flashover voltage showed higher values than at ℓ =1 and 2 cm. On the other hand, in the case of Thw, the luminosity showed similar properties to those of air. The 50% flashover voltage decreased abuot 5～10 kV when compared with the case of Ths and showed very close values.

Fig. (7) shows the breakdown characteristics of O_2. The state of luminosity is quite different from air and N_2. Broard luminosity was hardly observed at any gap voltage. As shown in Fig. (8), frequent observation of filamentary luminosity occupied the gap. The 50% flashover voltage depends on the gap length and showed distinctive values at each gap length. Also in this case, the 50% flashover voltage at ℓ =3 cm showed the highest value compared with at ℓ =1 and 2 cm. On the other hand, in the case of Thw, the luminosity was similar to Ths. The 50% flashover voltage under Thw showed about 5 kV lower than Ths.

THe following are the salient results obtained from the experiment.

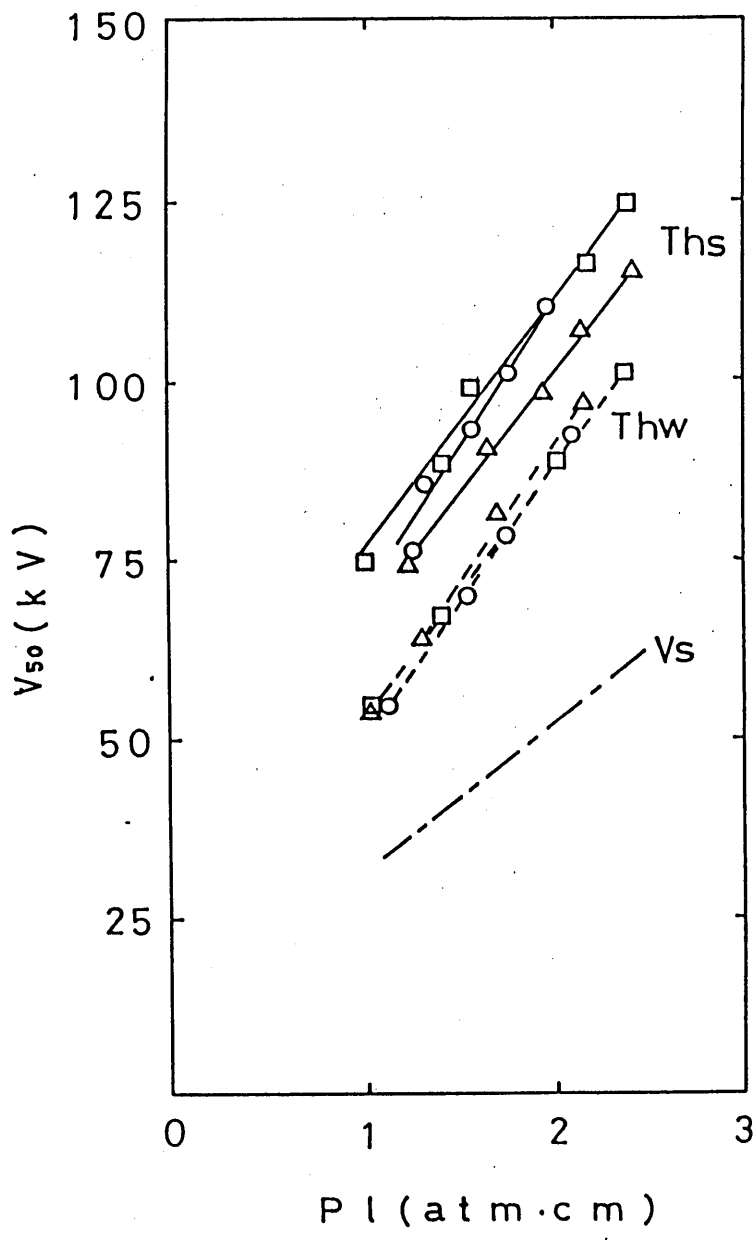

Fig. 7 50% flashover voltage vs pℓ characteristics of O_2

□ : ℓ = 3 cm, △ : ℓ = 2 cm, ○ : ℓ = 1 cm

Ths: Impulse waveform (10.8×30 ns)

Thw: Impulse waveform (10.8×74 ns)

V_s : Static breakdown voltage

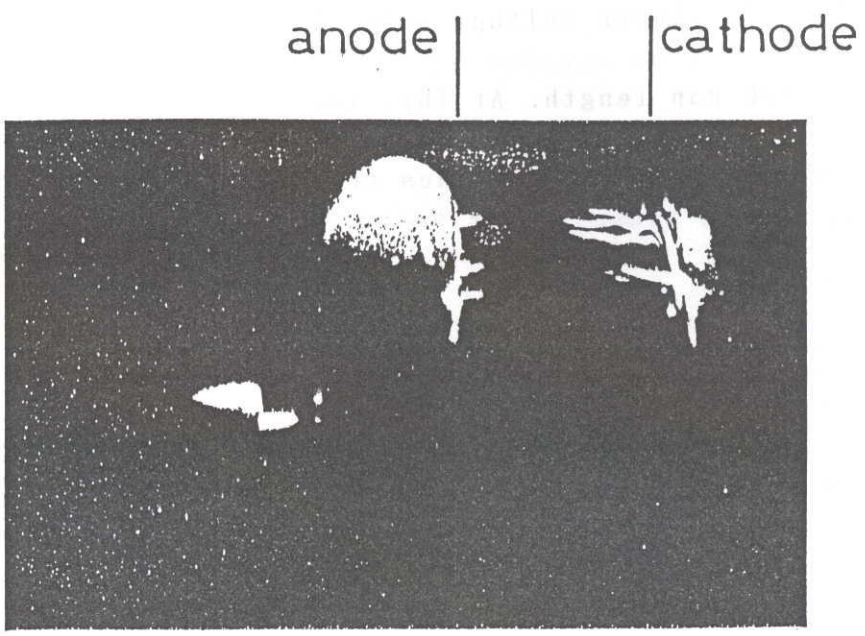

Fig. 8 Photographic evidence (state of filamentary luminosity)

(1) The 50% flashover voltage obtained at ℓ =1 and 2 cm showed very close values to each other in air and N_2 under impulse voltage with Ths. The 50% flashover voltage at ℓ =3 cm showed higher values than at ℓ =1 and 2 cm.

(2) The 50% flashover voltage under Ths in O_2 showed different values at each gap length. At Thw, the 50% flashover voltage, however, showed very close values to each other.

4. Discussion

4.1 Validity of Paschen's law

In the atmospheric gases of air, N_2 and O_2, the author has examined the breakdown characteristics of gas-insulated gaps by applying impulse voltages with durations of 30 and 74 ns, which had an influence on streamer formation. At static breakdown, the static breakdown voltage, V_s, is expressed as a function of $p\ell$. It is also the purpose of this article to see if Paschen's law is applied or not when nanosecond pulse voltages are applied

to gas-insulated gaps.

As a result, in the case of Ths in air and N_2, the 50% flashover voltage vs. $p\ell$ characteristics for ℓ =1 and 2 cm, showed very close values to each other. These experimental data show the validity of Paschen's law under the test conditions employed. At ℓ =3 cm, however, the 50% flashover voltage vs. $p\ell$ characteristics are different from the other data (at ℓ =1 and 2 cm). The flashover voltage for a given $p\ell$ is higher and an influence of gap length was observed.

On the other hand, in the case of Thw, the 50% flashover voltages at ℓ =1, 2 and 3 cm, were very close to each other. This means that Paschen's law is valid in the case of Thw under the test conditions employed.

In the case of Ths in O_2, the 50% flashover voltage differed at each gap length and Paschen's law does not seem to be applicable. In the case of Thw, however, a difference of flashover voltage due to gap length has not been observed and Paschen's law is applicable.

Validity of Paschen's law means that flashover voltage of the gap can be determined by $p\ell$, (i.e. $p\ell = nkT\ell = Kn\ell$)

where n: number density of molecules

k: Boltzmann's constant

T: temperature of gas

K: constant

the number density of molecules of the gap times gap length. In other words, the electron's energy obtained in a mean free path represents occurence of a flashover. From a physical point of view, the process of electron avalanche to streamer and to spark, can occur if the streamer criteria is satisfied by the space-charge field due to an electron's cloud ahead of electron avalanche. If

$$(\alpha - \eta) \chi = 20 \quad \text{in} \quad \exp \{ (\alpha - \eta) \chi \}$$

where α ; ionization coefficient

η ; attachment coefficient

χ ; developing distance of electron from cathode

A streamer starts to develop and it can be developed into flashover in a uniform field. The data shows that in spite of short impulse voltages such as 30 and 74 ns, the conventional avalanche-to-streamer theory seems to be applicable to the gaps. The property that the 50% flashover voltage obtained under Thw is lower than Ths is associated with the voltage duration of the impulse voltage used. It is also easily understood that flashover voltage to be obtained under infinite voltage duration becomes Vs.

On the other hand, it is observed that Paschen's law is not applicable at ℓ =3 cm under Ths. Streamer formation and its development depend on the gap length. A breakdown mechanism, different from that at ℓ =1 and 2 cm, may be required.

4.2 Investigation of the breakdown mechanism

The author has investigated the breakdown mechanism of gas-insulated gaps by nanosecond pulse application. The investigation is restricted to air because of insufficient experimental data on breakdown in the regime of large $p\ell$ in other gases. Prior to the application of conventional avalanche-to-streamer theory, it is timely to show the following experimental formula and criteria as

a first approximation.

(1) The following formula[11] is applicable between ionization coefficient, pressure, and field: E,

$$\alpha/p = 1.16 \times 10^{-4} \left(E/p - 28.0 \right)^2$$

(2) Electron's drift velocity[12]: v_e

$$v_e = 1.25 \times 10^7 \times \left(E/p/40 \right)^{1/2}$$

(3) Streamer criteria[11]

$$\alpha \chi = 20$$

The author calculated α, v_e, t_e (transit time of an electron

across the gap) and χ on the basis of a 50% flashover voltage vs. $p\ell$ characteristics obtained in air by using the above formula and criteria.

The results are listed in table I (maximum and minimum values are reported). t shows the transit time of electrons across χ and is obtained by $t = \chi / v_e$.

The results show that an electron emitted from cathode in the case of ultra high-field gaps satisfy the streamer criteria within developing distance of the electron, 0.048～0.18 cm and can develop into streamer. It is also shown in the table that in order to satisfy the streamer criteria for Ths, several nanoseconds are required after reaching peak value of the voltage. In the case of Thw, about ten nanoseconds are required after reaching peak value of the impulse. Breakdown of the gap may be caused by bridgeover of the streamer. On the streamer development and bridgeover, photographic observation by Image Converter Camera has shown the same phenomena of the gap. Details are scheduled to be reported in a second article.

	Ths	Thw
ℓ = 1 cm	α = 420-544 χ = 0.048-0.037 cm t = 2.43-2.0 ns	α = 208-319 χ = 0.096-0.063 cm t = 5.6-3.76 ns
ℓ = 2 cm	α = 203-262 χ = 0.099-0.076 cm t = 5.3-4.28 ns	α = 116-135 χ = 0.172-0.148 cm t = 9.6-9.1 ns
ℓ = 3 cm	.....	α = 88.4-109 χ = 0.23-0.18 cm t = 13-10.7 ns

Table 1 α , χ , t , values under Ths and Thw

5 Conclusions

Nanosecond pulse breakdown of gas-insulated gaps were investigated in air, N_2, and O_2. Conventional avalanche-to-streamer theory is applied to explain the breakdown mechanism.

The following describes salient conclusions:

(1) Under impulse voltage with half peak width, 30 ns, Paschen's law may be applicable in air and N_2 at gap length, ℓ =1 and 2 cm. At ℓ =3 cm, the 50% flashover voltage showed higher values than at ℓ =1 and 2 cm. Conventional avalanche-to-streamer theory may be applicable to explain the breakdown mechanism associated with ℓ =1 and ℓ =2 cm. Further investigation is required to explain the phenomena at ℓ =3 cm.

(2) Under impulse voltage with half peak width, 30 ns, in O_2, the 50% flashover voltage showed different values at each gap length and Paschen's law may not be applicable to this gap. Including physical coefficient of electron attachment, further investigation is required to analyze the phenomena.

(3) Under impulse voltage with half peak width, 74 ns, Paschen's law may be applicable in air, N_2, and O_2 at each gap length.

(4) In the case of the ultra high field gaps in these tests, I showed that an electron emitted from the cathode satisfied streamer criteria

within developing distance of the electron, 1.8 mm and can develop into streamer, causing flashover.

References

1. L. B. Loeb, Fundamental Process in Electrical Discharge in Gases, John Wiley and Sons, Inc., New York (1939)

2. J. M. Meek and J. D. Craggs, Electrical Breakdown of Gases, Oxford, Clarendon Press, (1953)

3. H. Raether, Electron Avalanches and Breakdown in Gases, Butterworths, London (1964)

4. E. E. Kunhardt and W. W. Byszewski, Development of overvoltage breakdown at high gas pressure, Phys. Rev. A 21, pp.2029-2076(1980)

5. A. V. Gurevich, On the theory of runaway electrons, Soviet Phys. JETP, 12, pp.904-912(1961)

6. L. P. Babich and Yu. L. Stankevich,
Transition from streamer to continuos electron accelaration,
Soviet Phys. Tech. Phys. 17, pp.1333-1336(1973)

7. Y. Kubota, S. Kawasaki, A. Miyahara and H. M. Saad,
Coaxial Marx generator for producing intense relativistic electron beams,
Jpn. J. Appl. Phys.. 13, pp.260-263(1974)

8. Y. Kubota, J. Kodaira and A. Miyahara,
Study of the rectangular-like output waveforms of a 720 kV coaxial Marx generator,
Jpn. J. Appl. Phys, 20, pp.2397-2400(1981)

9. Y. Sakato, T. Hashimoto, M. Obata and T. Fugioka,
Low-impedance, coaxial-type Marx generator with a quasi-rectangular output waveform,
2nd IEEE international pulsed power conference digest of papers,
Lubbock, TX, USA, pp.165-171 June 1979

10. H.Matsuzawa and T. Akita,

Output voltage waveform improvement of the coaxial Marx-type high-voltage generator,

Rev. Sci. Instrum, 56(12), pp.2287-2289(1985)

11. K. Honda,

On a streamer breakdown criterion of a uniform air gap,

J. I. E. E. J. 85, .pp.116-123(1965)

12. H. Raether,

Über den aufbau von gas entladungen.

Z. Phys., 117. pp.375-398(1941)

Chapter III Breakdown Phenomena of Gas-Insulated Gaps With Nanosecond Pulses*

1 Introduction

Two basic models have been proposed to explain the initial phase of electrical breakdown in gases.[1,2] These are commonly known as the Townsend avalanche model and the streamer model. Although electron emission from the cathode is, of course, required to initiate flashover, the main difference from Townsend's theory is that a discharge can develop regardless of ν (electron emission from cathode by secondary mechanism) at the initial stage of breakdown dominated by an applied electrostatic field. This is an essential difference between Townsend's theory and

* Publication in the 1 January 1989 issue of the Journal of Applied Physics { J. Appl. Phys. 65, 51 (1989) }

the streamer theory. The regime of validity of these models, however, is not clear because of their complexty.

On the other hand, it is generally understood that impulse voltage breakdown shows different properties depending on rise time and pulse duration. For the purpose of clarifying the streamer formation and its development, an examination of $p\ell$ (p: pressure, ℓ : gap length) versus flashover characteristics, using impulse voltages with short duration, was carried out under the illumination of weak ultraviolet rays (mercury lamp, with an output of 10 W , main spectrum 2537A and 1849 A) on the entire surface of the cathode[3]. The previous article showed that the 50% probability of flashover voltage versus $p\ell$ characteristics was exlained by Paschen's law for air, N_2, and O_2 at gap lengths ℓ =1 and 2 cm. Conventional avalanche-to-streamer theory was then used to explain the breakdown mechanism.

After the previous experiments, the author obtained breakdown data for several kinds of gases that were subjected to impulse voltages (10.8 × 30 ns) using the spot illumination of the weak ultraviolet rays on the cathode surface. Breakdown properties such as 50% probability of flashover voltage and physical appearance, i.e., luminosity of a gas

between the illumination on the entire surface of the cathode and the spot illumination on the cathode, were investigated.
In addition to this data, the modified experimental apparatus enabled the author to observe the time lag of the flashover.

This article describes experimental results such as 50% probabil of flashover voltage of gas-insulated gaps in air, N_2 and O_2, the property of luminosity by still camera photography; and the observed time lag of flashover and its flashover probability distribution. Moreover, the author attempted to investigate the streamer formation on the basis of the conventional avalanche-to-streamer theory and tim lag characteristics observed.

2 Apparatus

The diagram of this experimental circuit and data acquisition system is shown in Fig.(1). The high-voltage impulse generator used in this study is a coaxial Marx-type generator. Maximum output voltage is 130kv and is set by the charging voltage of the Marx generator and

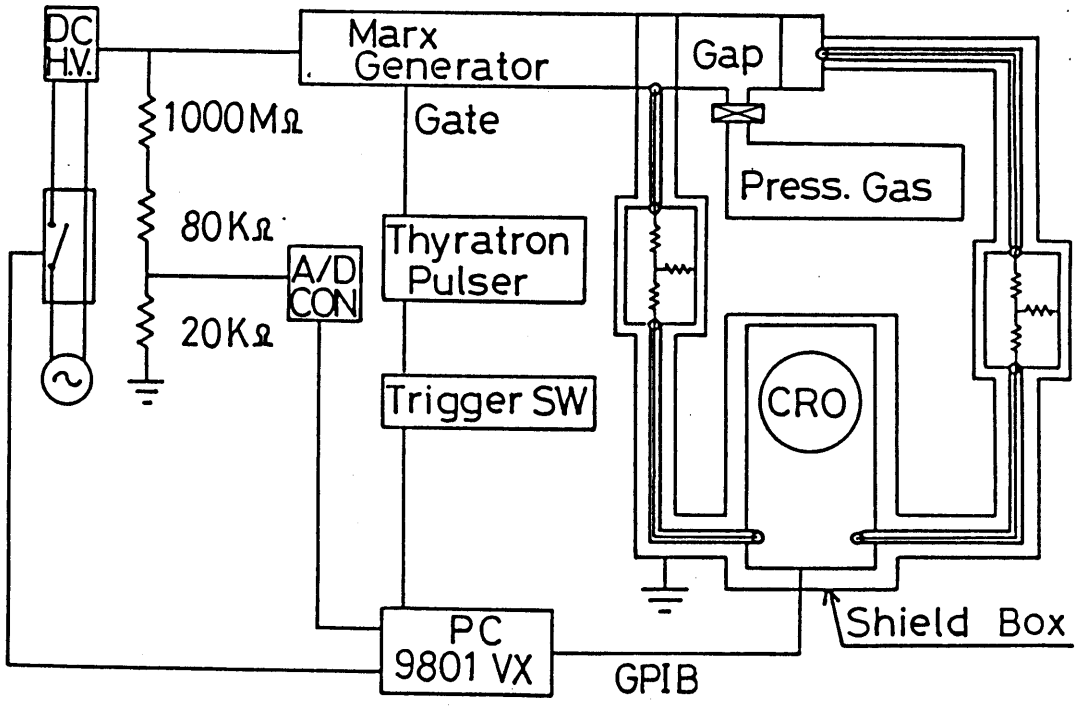

Fig. 1 Experimental circuit arrangement and data acquisition system

its output resistor($CuSO_4$ solution).

Uniform test gaps used in this test are stainless steel Rogowski -shaped electrodes with a diameter of 9 cm. For the test, the stainless container in which the test gaps are located was evacuated to 10^{-5} Torr using rotary and diffusion pumps. Various gases such as air, N_2 and O_2 were then backfilled into the container to the desired pressure. To minimize the fluctuations of flashover voltage, as shown in Fig.(2), ultraviolet rays were continuously applied to the cathode surface through the 1-mm-diam hole located in the center of the anode. Each shot was separated by 1-min intervals to allow the experiment to stabilize.

The impulse voltage wave shape was recorded by Iwatsu storage oscilloscope (TS-8123) from the $CuSO_4$ solution as a resistance divider monitor. The cathode is grounded by the $CuSO_4$ resistor to permit the flashover discharge current to be observed.

The measurements for obtaining waveforms of impulse voltages and currents were made in a steel-reinforced concrete walled room to reduce the noise generated by the high voltage source. In addition, the storage oscilloscope was installed inside a Faraday cage made of copper plate.

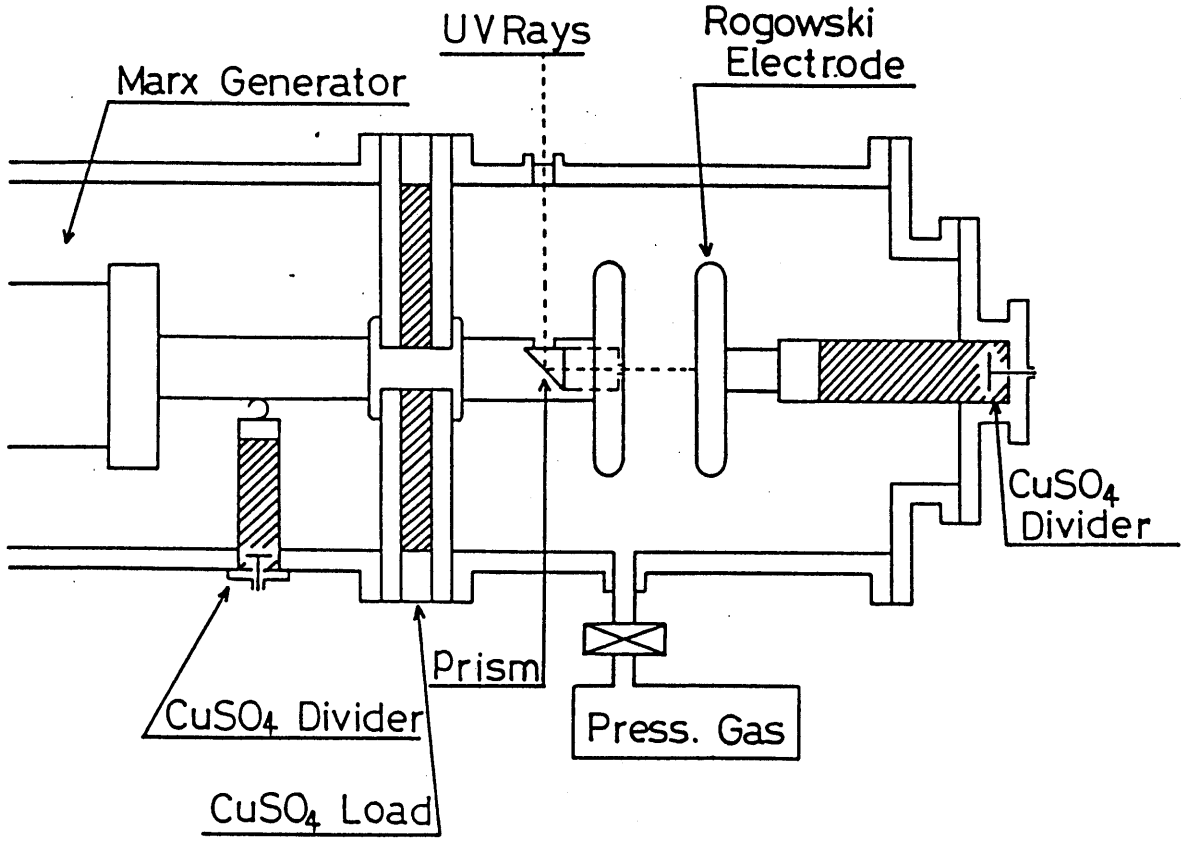

Fig. 2 Test gaps and illumination method of ultraviolet rays

All connecting coaxial cables were placed inside copper tubes to minimize the electrical noise. The impulse voltage and discharge currents were statistically analyzed by a computer. An impulse waveform used during this test is shown in Fig.(3). Rise time of 10.8 ns and pulse duration at half peak of 30 ns are obtained.

3 Experimental Results

The author will now describe the breakdown properties of various gases such as air, N_2 and O_2 in uniform fields for the case of the spot illumination of the ultraviolet rays on the cathode surface.

3.1 50% probability of flashover voltage

Figures (4) to (7) show the breakdown characteristics of various gases. V_{50} means 50% probability of flashover voltage and is obtained by an interpolation method. In this paper and the previous article[3],

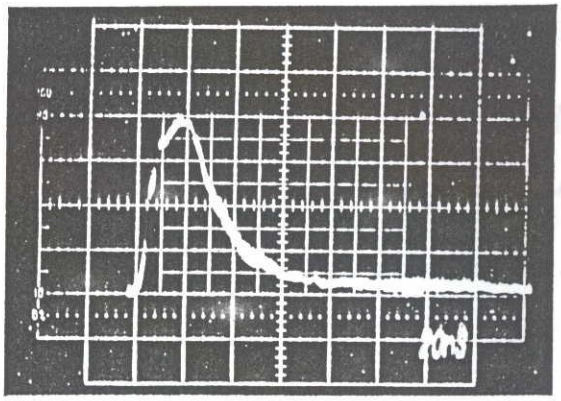

Fig. 3 Impulse waveform

flashover characteristics are reported using the parameter $p\ell$, which represents the energy an electron obtains in a mean free path of a gas.

Fig. (4) shows breakdown characteristics of air. In this figure, V_s indicates static sparking voltage of the gap. As $p\ell$ increases, the 50% probability of flashover voltage linearly increases. At ℓ =1 and 2 cm, their characteristics are quite similar, and the 50% probability of flashover voltage is statistically the same within ± 5%.
The 50% probability of flashover voltage with spot illumination provided data values similar to those obtained by illumination on the entire surface of the cathode[3]. No difference of flashover voltages has been observed in either illumination method.

On the other hand, the examination of luminosity by still-camera photography showed that broad luminosity[3], observed in the case of the illumination of the ultraviolet rays on the entire surface of the cathode, was not observed for spot illumination of the gap conditions of ℓ =1 and 2 cm and pressures between 380 and 1440 Torr. Only blue-white filamentary luminosity appeared when the flashover occurred. Fig. (5) shows a photograph of the filamentary luminosity.

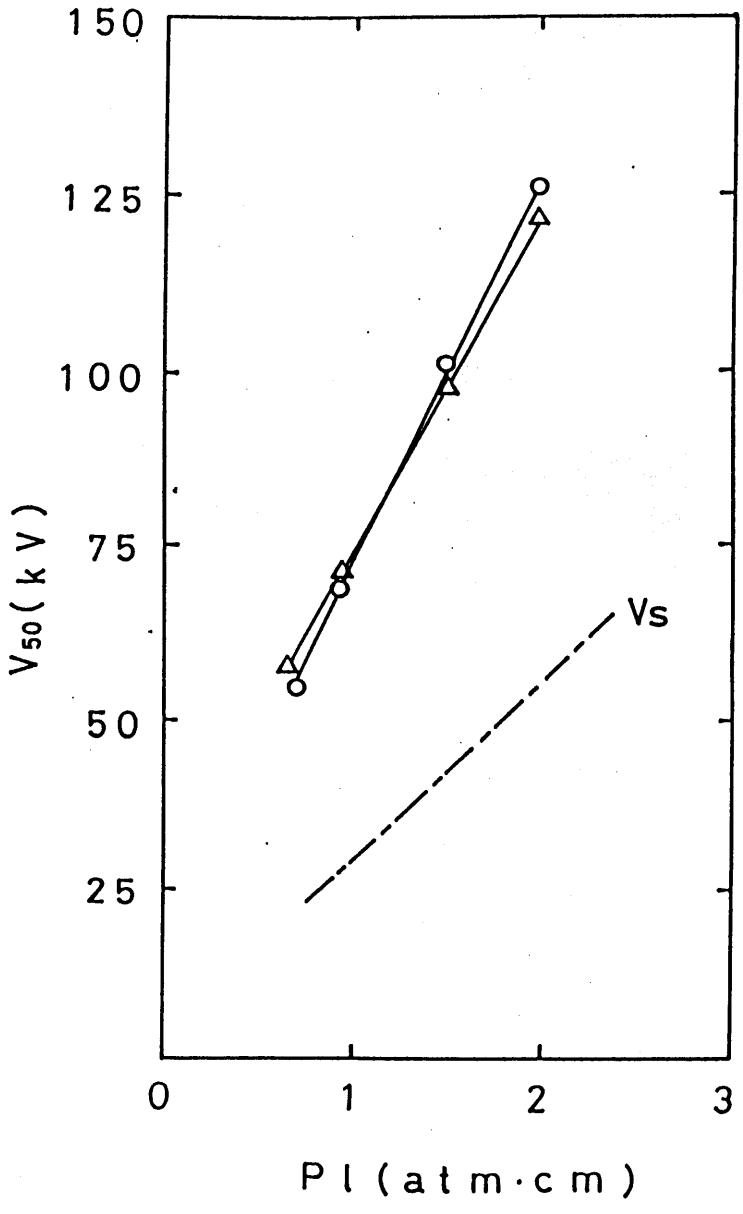

Fig. 4 50% probability of flashover voltage vs pℓ characteristics of air

△: ℓ = 2 cm, ○: ℓ = 1 cm

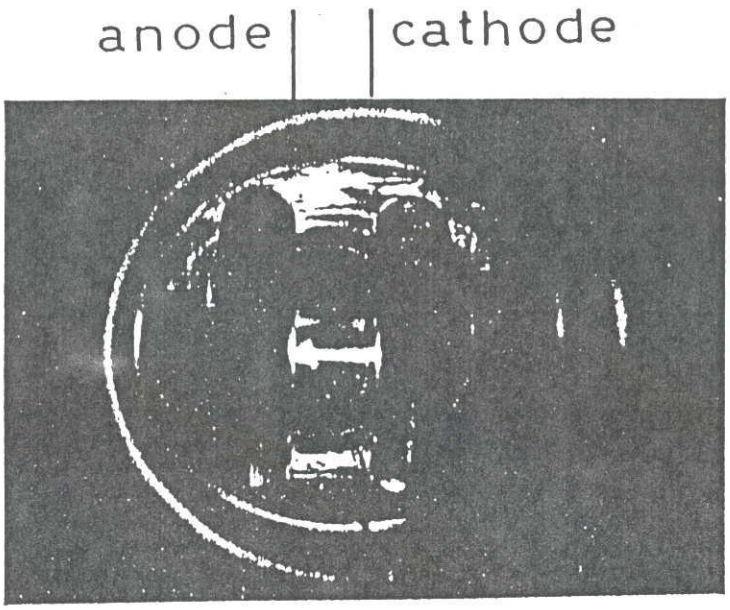

Fig. 5 Photographic evidence of the state of filamentary luminosity

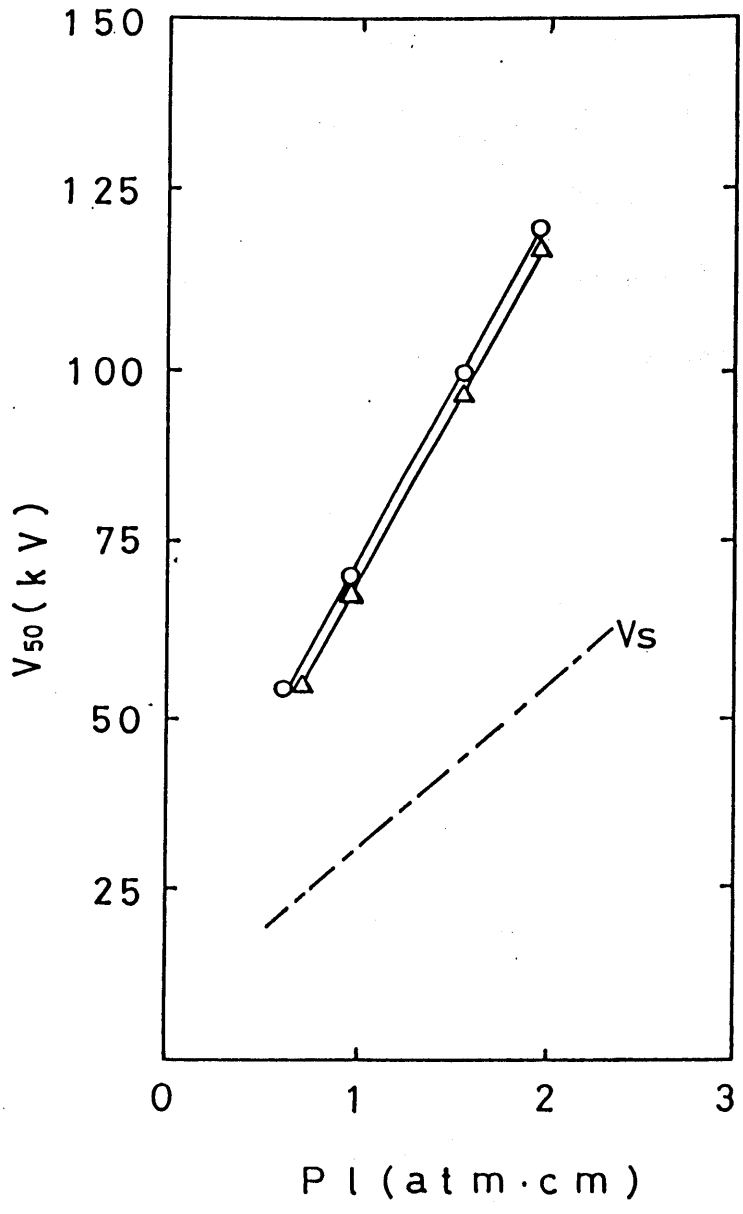

Fig. 6 50% probability of flashover voltage vs pℓ characteristics of N_2

△: ℓ = 2 cm, ○: ℓ = 1 cm

Fig. (6) shows breakdown characteristics of N_2. The 50% probability of flashover voltage is closely correlated for both gap lengths and increases linearly with increasing $p\ell$ values. In the case of the spot illumination using ultraviolet rays in N_2, broad luminosity has not been observed for these gap conditions. The author also observed that there are no distinct differences in the 50% probability of flashover voltage between entire illumination and spot illumination.

Fig. (7) shows breakdown characteristics of O_2. In the case of the spot illumination on the cathode, the filamentary luminosity which disconnect in the middle of the gap, as reported in the previous article[3], has not been observed. Flashover in the case of the spot illumination occurred without such restraint of the streamer.

The 50% probability of flashover voltage increases lineary with increasing $p\ell$ values and shows very close values at each gap length. The author observed that there was no difference in the flashover voltage between spot illumination and entire illumination.

Breakdown characteristics by impulse voltage of various gases such as air, N_2 and O_2 were examined under the spot illumination of the ultraviolet rays on the cathode. The following are the salient results.

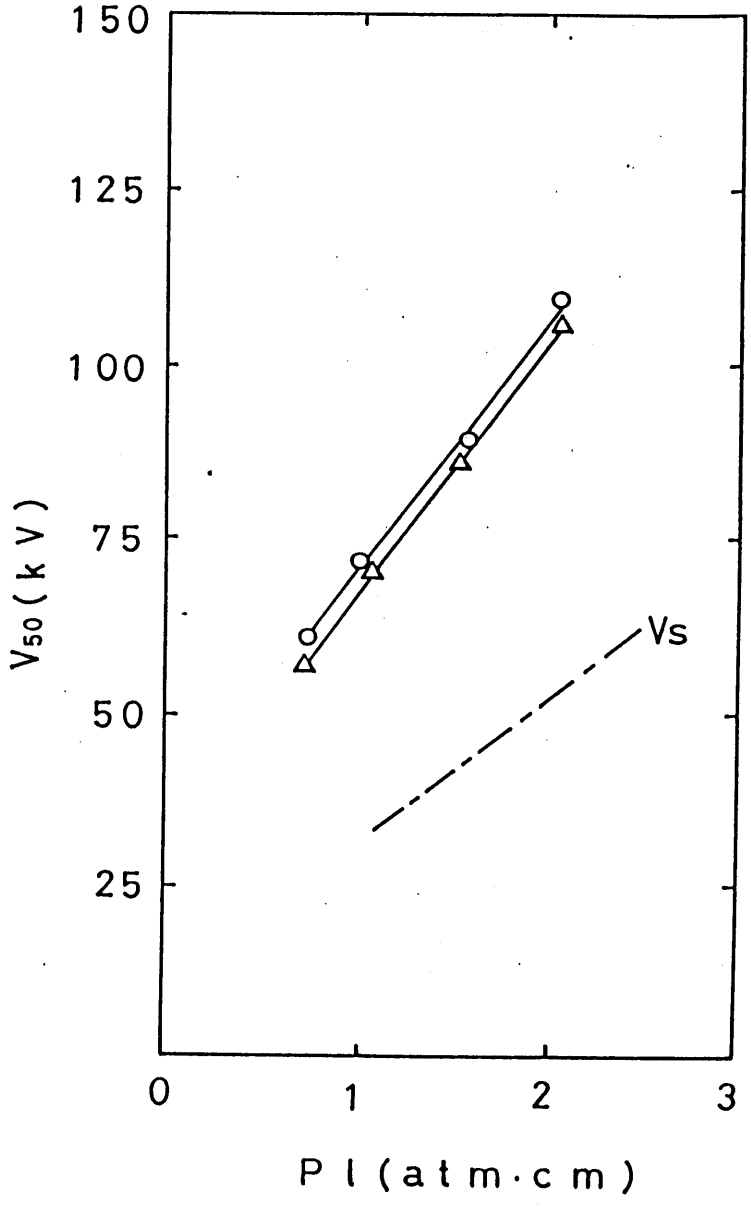

Fig. 7 50% probability of flashover voltage vs pℓ characteristics of O_2

△: ℓ = 2 cm, ○: ℓ = 1 cm

(1) There is no difference in 50% probability of flashover voltage between the the spot illumination and the entire illumination on the cathode.

(2) Broad luminosity, observed in the case of the entire illumination on the cathode, has not been observed in the spot illumination for air and N_2. Streamer phenomena disconnect in the middle of the gap, observed in the entire illumination in O_2, have not been observed in the case of the spot illumination.

3.2 Observed time lag of flashover

To study the breakdown mechanism of the gas-insulated gaps, with nanosecond pulses, the time-lag properties of breakdown were examined.

Fig. (8) shows the typical relation between the applied impulse voltage and the discharge current waveform. The current waveform was triggered by the application of impulse voltage and these waveforms were recorded by the dual-beam oscilloscope. The discharge current

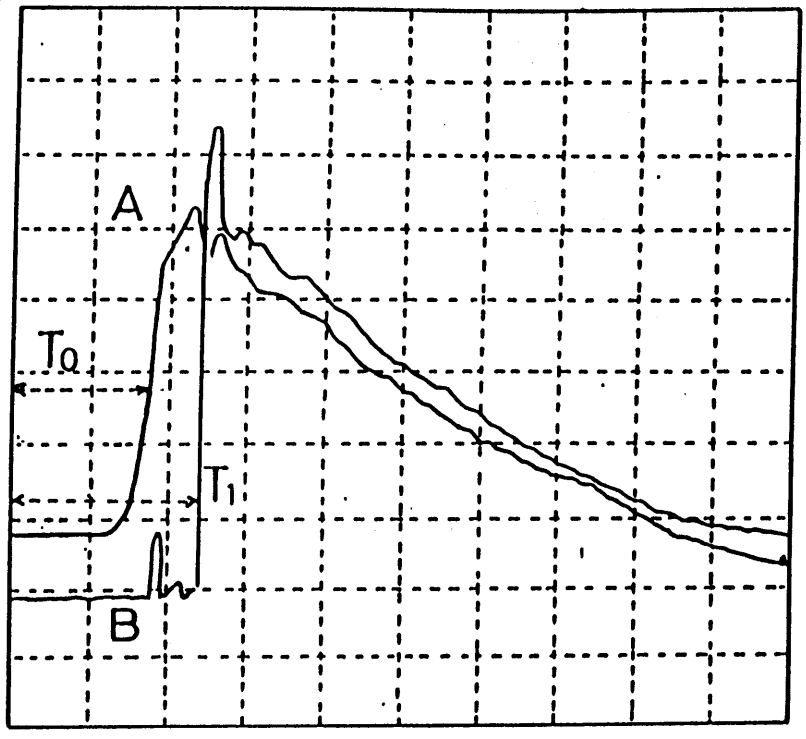

Fig. 8 Impulse voltage and discharge current waveforms

A: Applied impulse voltage

B: Discharge current

The unit is arbitrary

shows a rapid increase when the flashover occurrs. The T measured in these waveforms is the time lag. The time lag of the flashover is comparable to the rise time and the pulse duration and it is difficult to define a time lag. In this article, to allow analysis, the time lag is defined as follows: Time lag T_0 occurs when the incident voltage impulse exceeds a certain electric field, 23.8 kV/cm. This is the value of the electric field, which has $\alpha = 1$ at P= 760 Torr (calculated from formula (1), listed below) . Completed flashover occurs at T_1. The total time lag T can be expressed by the relation:

$$T=T_1-T_0$$

These T' s were computed by the data acquisition system and the probability density of the time lag was obtained for various gases. Fig. (9) to (17) show the relation between probability density and time delay for air, N_2 and O_2. The probability distribution was determined by a number of experiments. For each condition, one hundred shots provided the distribution. The transit time of the electrons required to satisfy the conventional streamer criteria is indicated in the same figures to study the formative time lag of flashover. The transit time calculation is restricted to air because of

insufficient experimental data on breakdown in the regime of large pℓ in other gases. The transit time of the electrons (T_t) was calculated by the numerical integration (trapezoidal rule) with the following three formulas, [4,5] and one relation form on the basis of the time-varying incident impulse voltage:

(1) $\alpha/p = 1.16 \times 10^{-4} (E/p - 28.0)^2$ (1)

α : ionization coefficient

p : pressure

E : applied field

(2) $v_e = 1.25 \times 10^7 \times (E/p/40)^{1/2}$ (2)

v_e : electron drift velocity

(3) $\int_0^{T_c} \alpha \cdot v_e \, dt = 20$ (3)

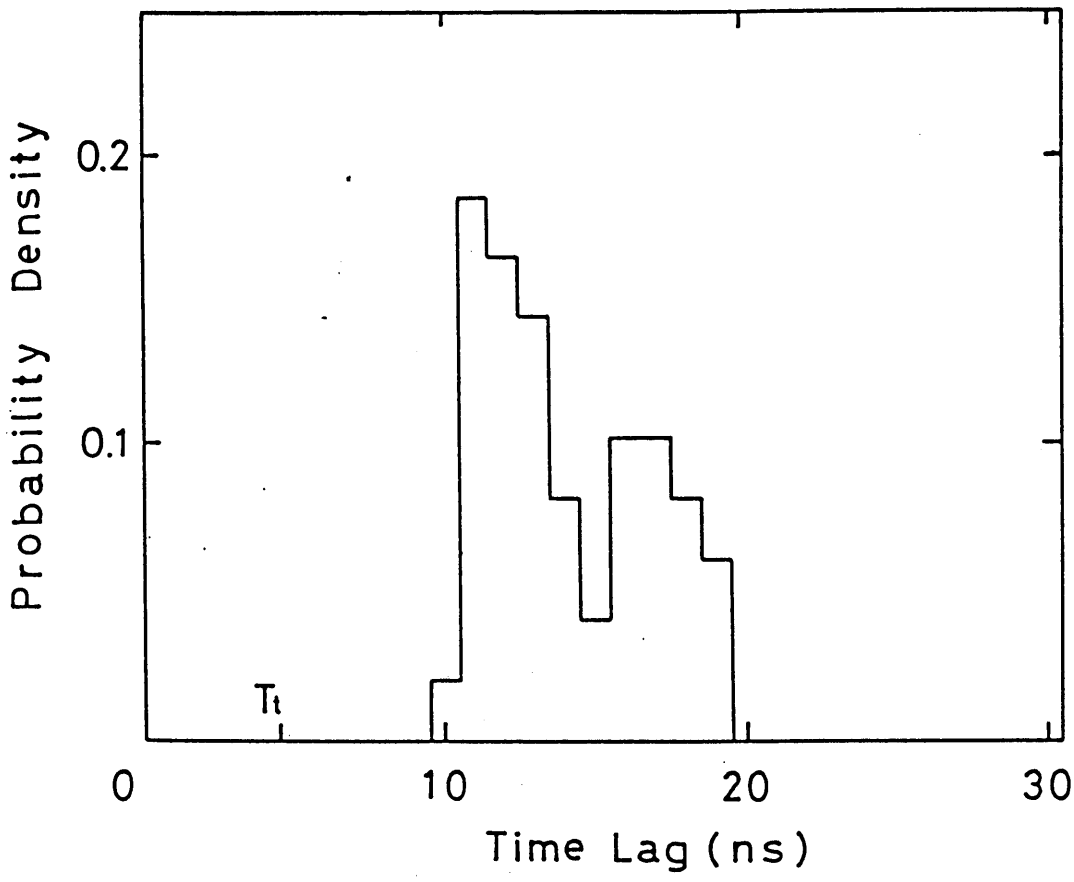

Fig. 9 Histograms of observational delay time

ℓ = 1 cm; air ; p= 760 Torr;

Applied voltage= 72 kV

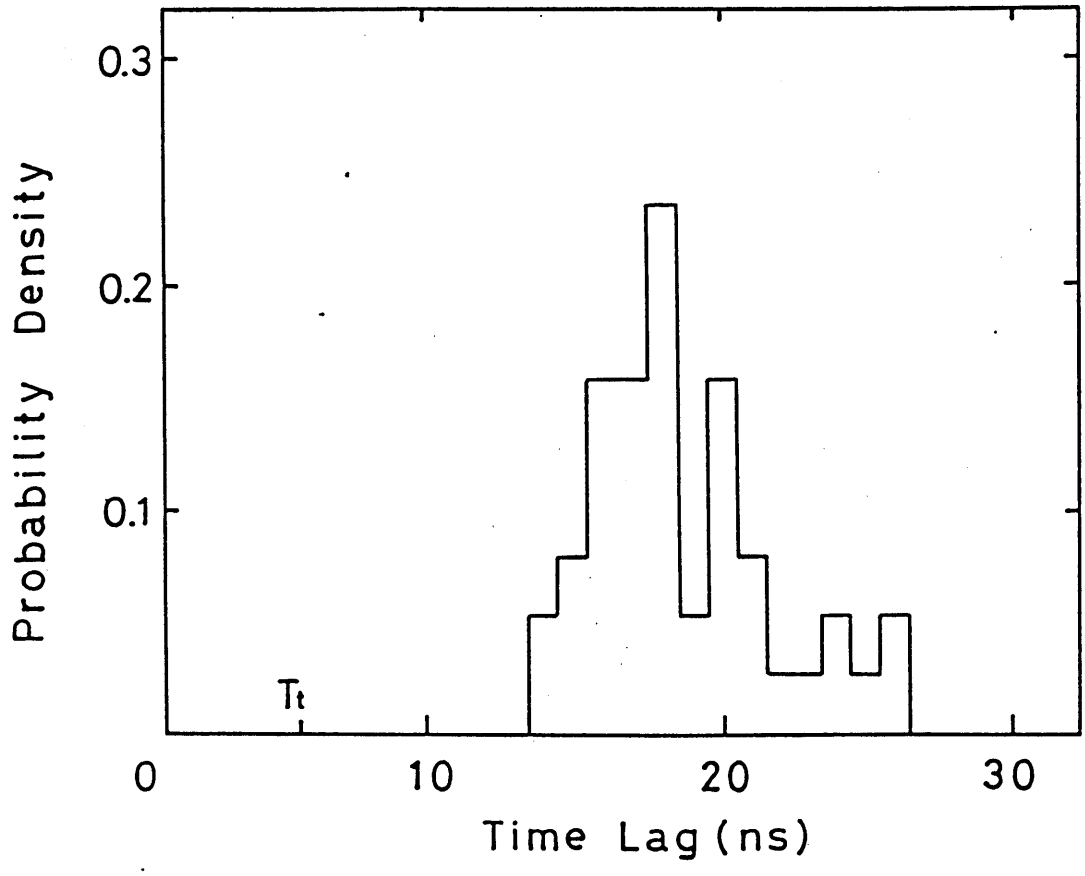

Fig. 10 Histograms of observational delay time

ℓ = 1.5 cm; air ; p= 760 Torr

Applied voltage= 110 kV

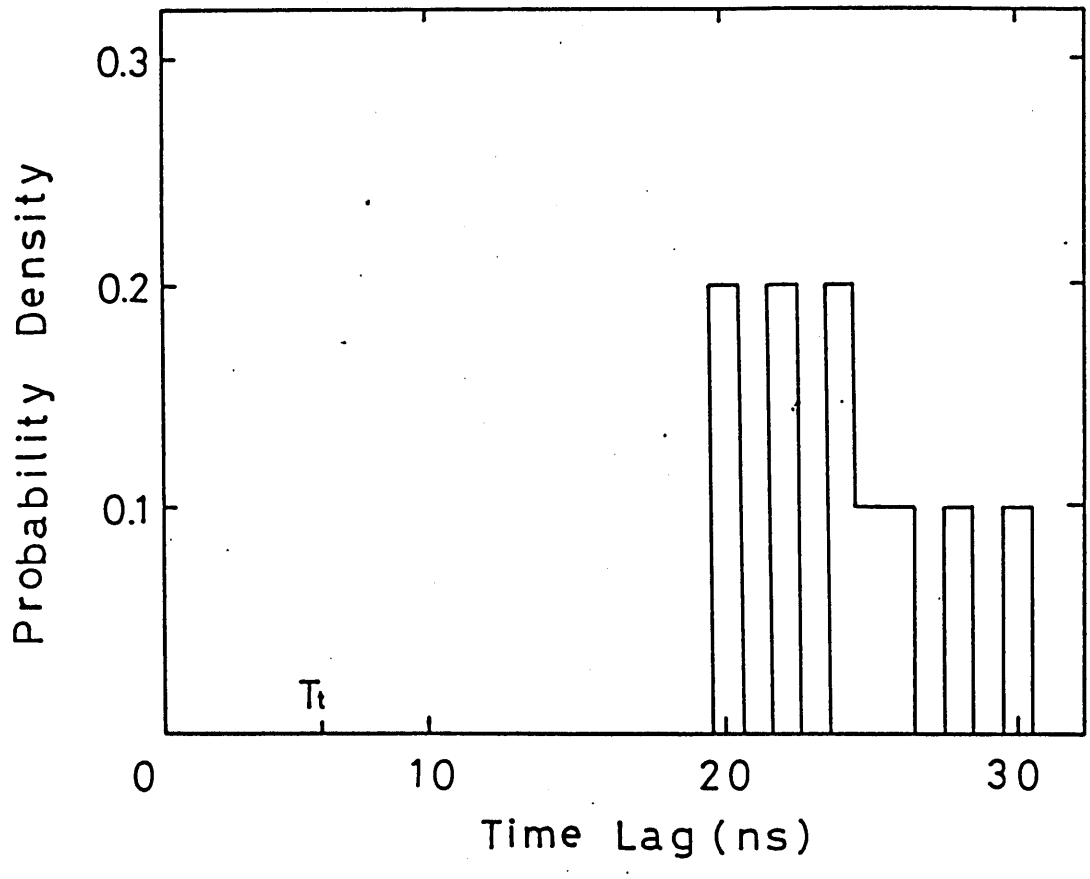

Fig. 11 Histograms of observational delay time

ℓ = 2 cm; air ; p= 760 Torr

Applied voltage= 125 kV

$T_t = T_o$ - time when the electric field exceeds 23.8 kV/cm from the application of impulse voltage[4] ; α is the ionization coefficient in cm^{-1} ; P is the pressure in mm Hg; E is the applied field in V/cm; and v_e is the electron drift velocity in cm/s; and t is the time in s.

Figs. (9) to (11) show the histograms of the distribution for air. Although measured time-lag values varied, the author observed that the minimum value of the distribution increases as the gap length increases. On the other hand, the calculated transit time T_t of the electron, shown in Figs. (9) to (11), does not coincide with the probability distribution, but is below the distribution . It is interesting that the difference between the actual minimum values and the calculated transit time becomes greater as the gap length increases.

Fig. (12) to (14) show the histograms of the distribution for N_2. The minimum value of the distribution increases as the gap length increases.

Fig. (15) to (17) show the distribution histograms for O_2. The probability distribution is quite different from air and N_2. The distribution for O_2 is strikingly narrower than for air and N_2. It is

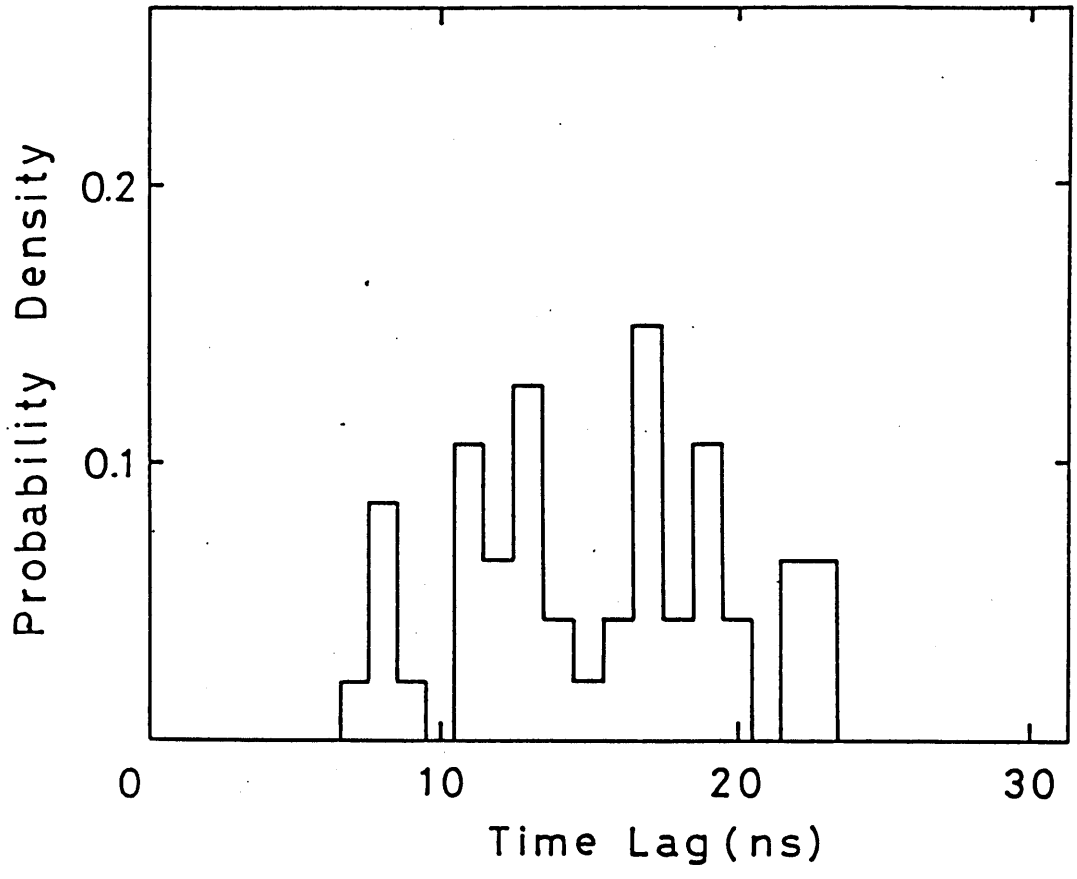

Fig. 12 Histograms of observational delay time

ℓ = 1 cm; N_2 , p= 760 Torr

Applied voltage= 68 kV

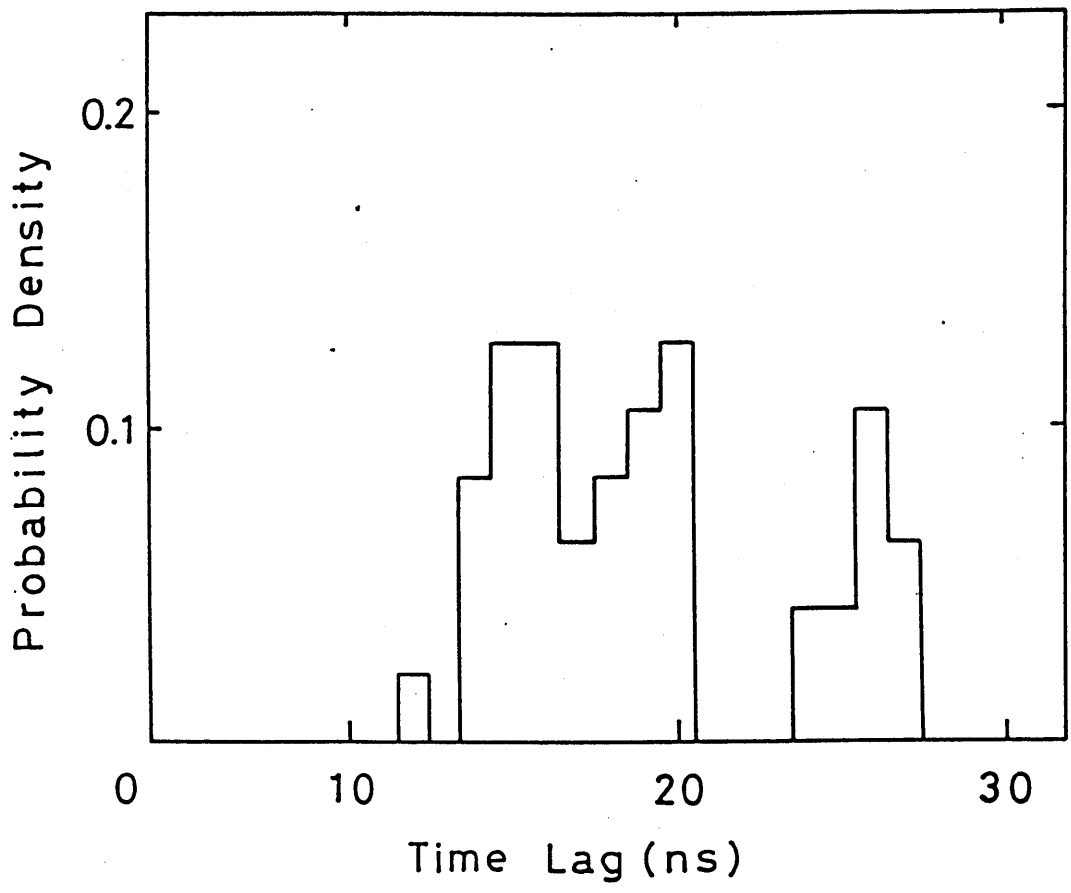

Fig. 13 Histograms of observational delay time

ℓ = 1.5 cm ; N_2 ; p= 760 Torr

Applied voltage= 110 kV

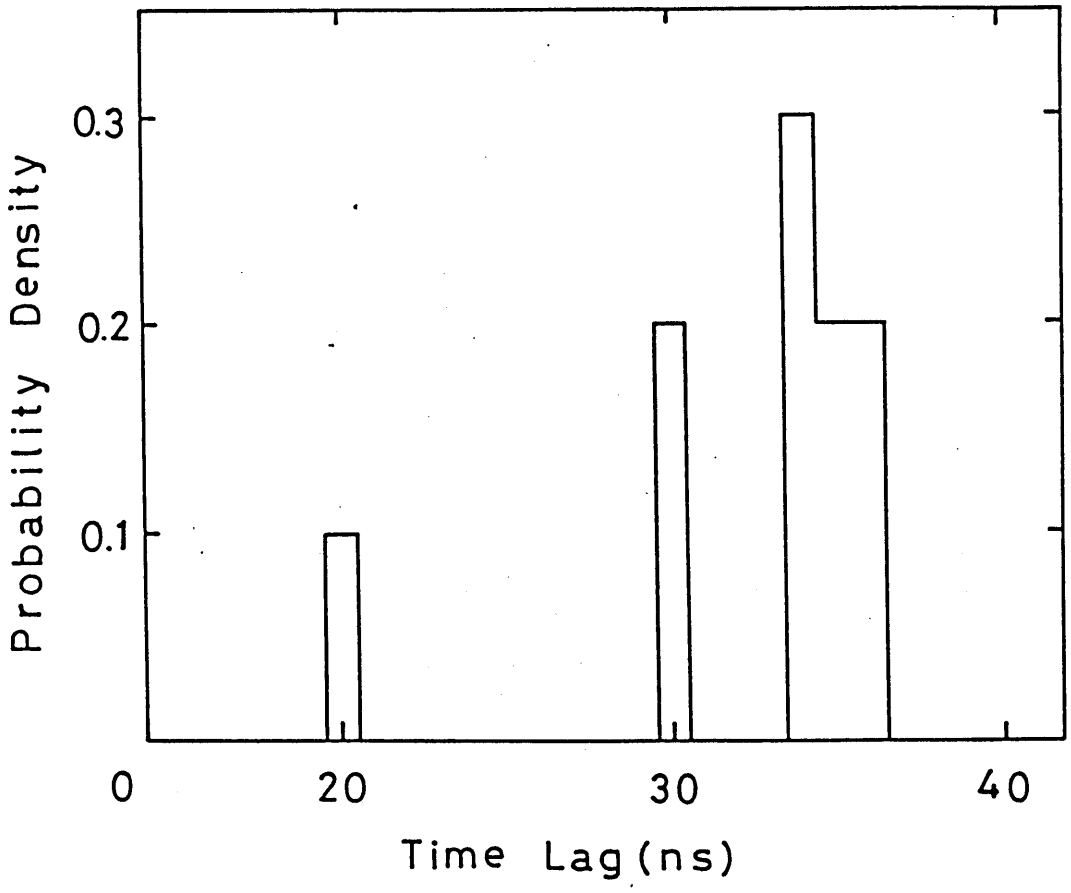

Fig. 14 Histograms of observational delay time

ℓ = 2 cm ; N_2 ; p= 760 Torr

Applied voltage= 130 kV

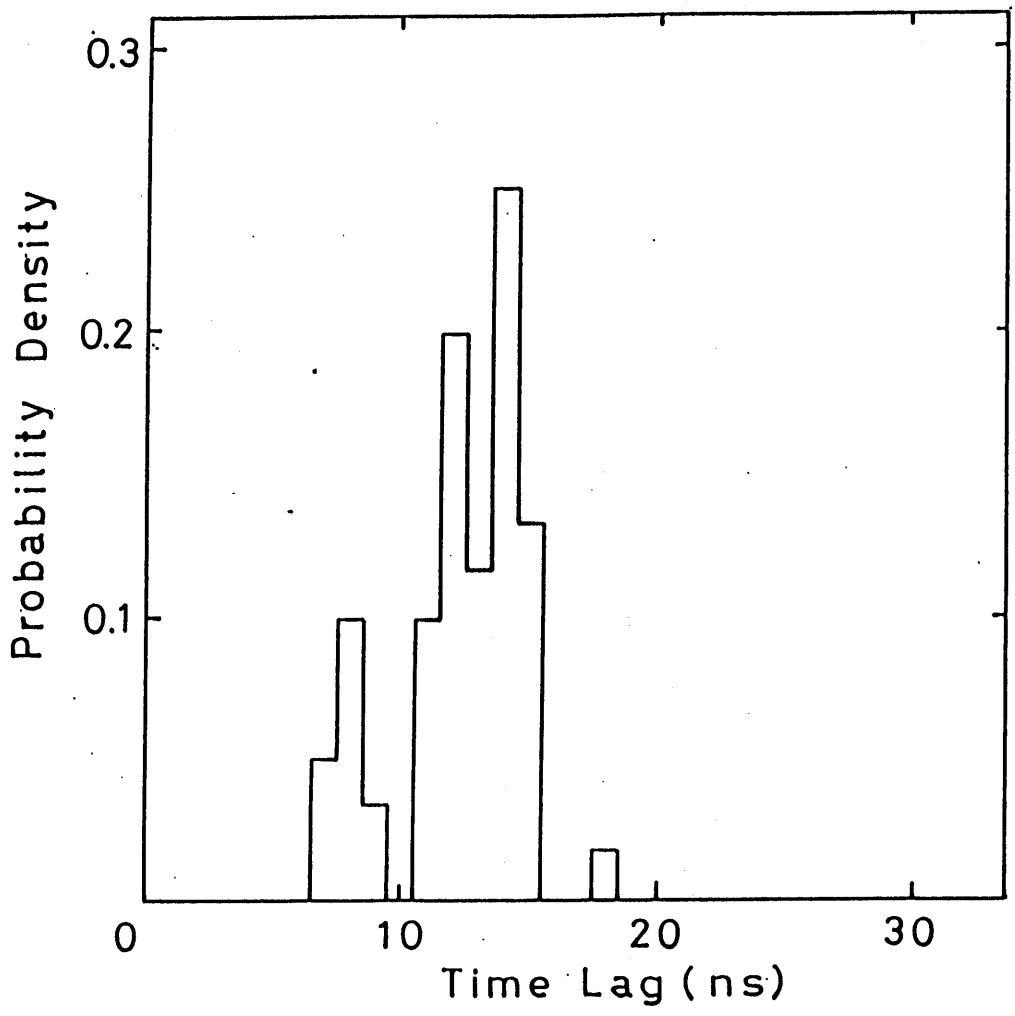

Fig. 15 Histograms of observational delay time

ℓ = 1 cm ; O_2 ; p= 760 Torr

Applied voltage= 68 kV

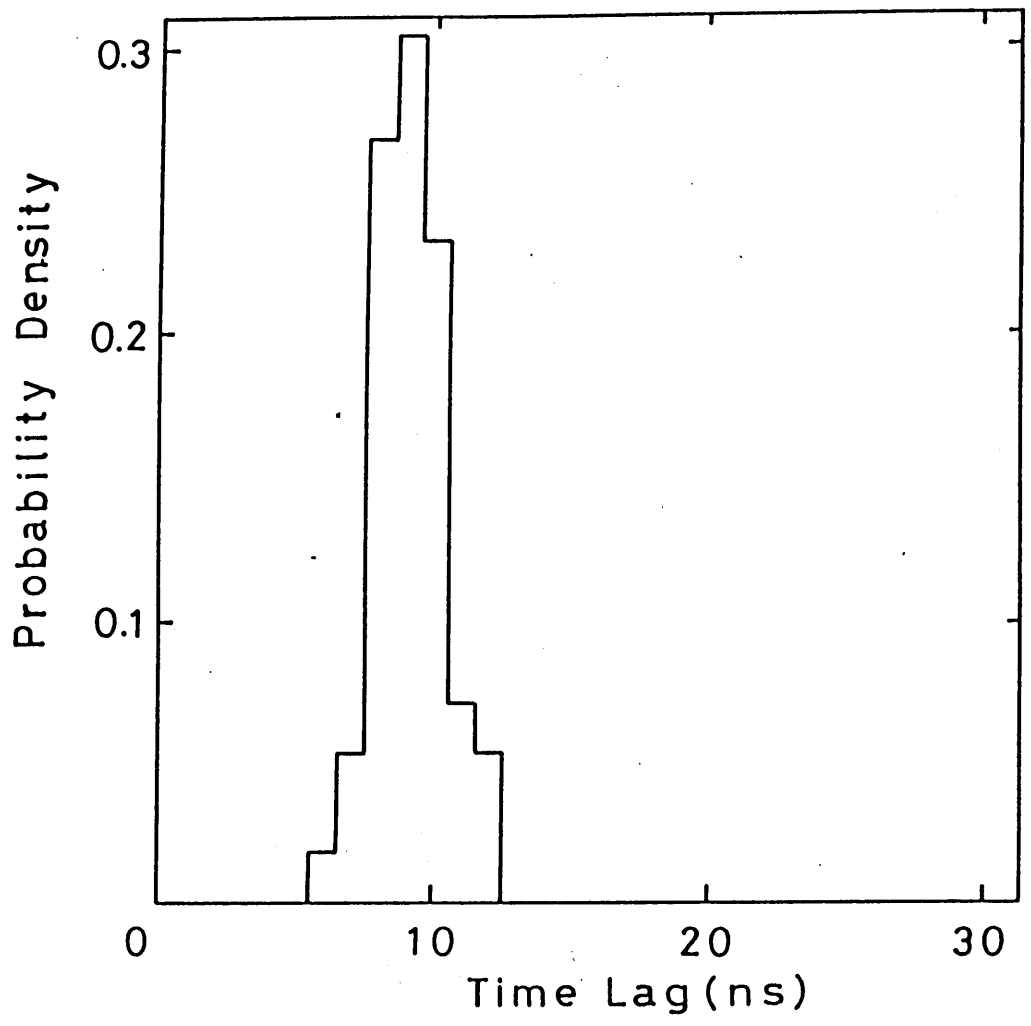

Fig. 16 Histograms of observational delay time

ℓ = 1.5 cm ; O_2 ; p= 760 Torr

Applied voltage= 93 kV

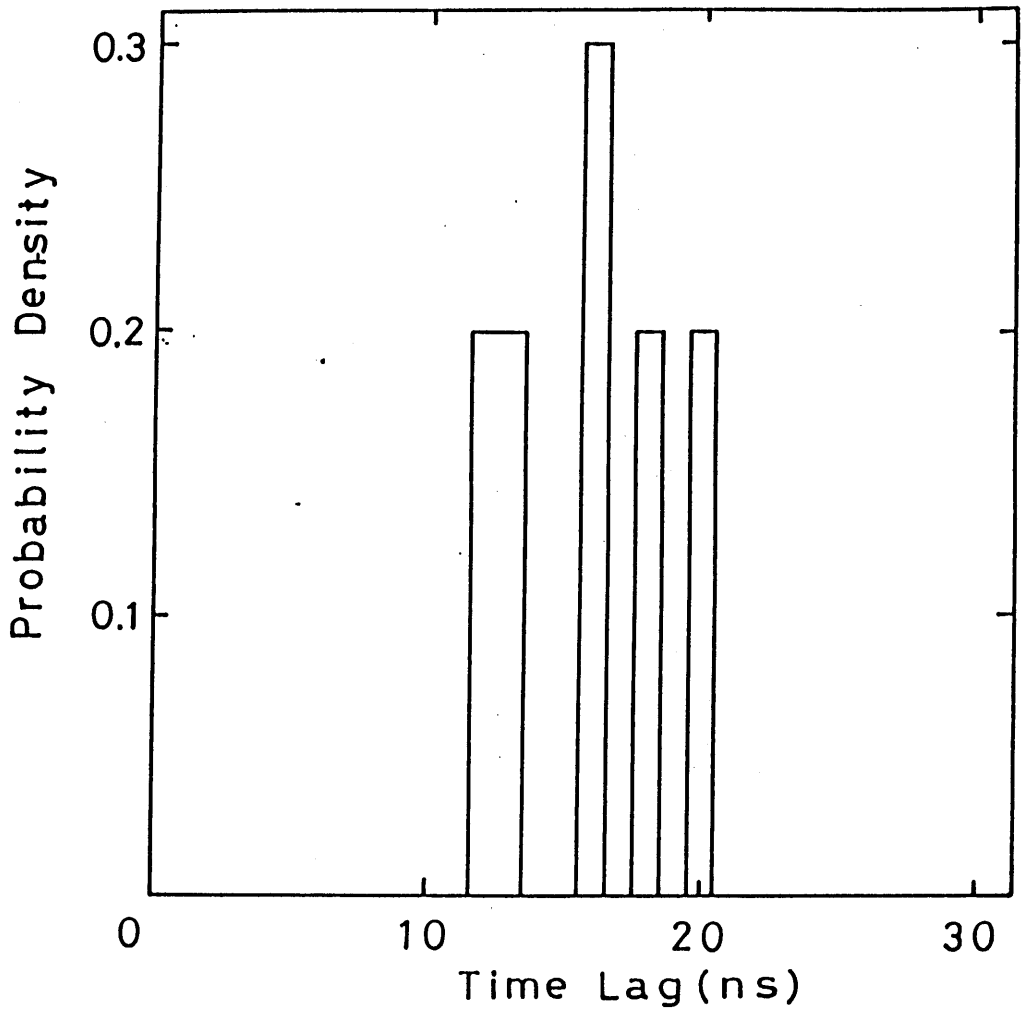

Fig. 17 Histograms of observational delay time

ℓ = 2 cm ; O_2 ; p= 760 Torr

Applied voltage= 113 kV

observed that the probability distribution for gap length ℓ =1, 1.5, and 2 cm , are quite similar to each other and do not depend on gap length.

In summary, the probability density of the observed time lag of flashover was examined for air, N_2 and O_2. The following are the salient results obtained from the experiment:

(1) The minimum time lag in the distribution for air and N_2 increases as the gap length increases. The calculated transit time of the electron to satisfy the conventional streamer criteria for air, however, does not coincide with the probability distribution; the calculated transit time is below the actual data distribution.

(2) The probability distribution for O_2 is quite different from air and N_2. The distribution is narrower and the probability density does not depend on gap length for the experimental parameter employed.

4.0 Discussion

The author has examined the breakdown characteristics of gas-insulated gaps in the atmospheric gases of air, N_2, and O_2 by applying 30-ns impulse voltages, to influence streamer formation. In the experimental results obtained, the observed time lag of flashover and the probability distribution are used to study the breakdown mechanism of these gas-insulated gaps. Application of the conventional streamer criteria by using the electron drift velocity helped the author to investigate the breakdown mechanism.

As indicated in Fig.(9) to (11), the calculated transit time of the electron across the distance, needed to satisfy the streamer criteria, is less than the distribution function.

It is well known that time lag consists of the formative time lag and the statistical time lag. From the probability distribution point of view (Laue plot), the minimum values obtained in the Laue plot is the formative time lag. The fact that the calculated transit time of the electron is below the data distribution on the lower side may be explained by considering the electron drift velocity and the streamer

velocity as follows: The electron emitted from the cathode by ultra -violet rays forms the avalanche in the gap with the time given above. The electrons produced by collision ionizations are located ahead of the electron avalanche. Positive ions are immobile where they are produced. If the number of the electrons exceeds a certain value, about 10^8, the electrons are more strongly attracted by positive ions, and conversion into plasma with high conductivity occurrs. The strong field ahead of the electron avalanche produces further avalanches around the avalanche head. This phenomena means the start of streamer. After the streamer develops, it has a velocity of the order of 10^8cm/s (Ref. 6) and contributes to the rapid increase of the current observed on the oscilloscope screen(T_1 in Fig.8)

On the basis of this electron drift velocity and streamer velocity, the author believes that the experimental results, such as the observed time lag of flashover and the probability distribution, can be explained by this model, and that the explanation is reasonable.

On the streamer development and bridgeover, photographic observation by an image converter camera has shown the same phenomena of the gap. Details are scheduled to be reported in the third article in this series.

5. Conclusions

Nanosecond pulse breakdown of gas-insulated gaps was examined using spot illumination from ultraviolet rays on the cathode surface. 50% probability of flashover voltage of gas-insulated gaps in air, N_2 and O_2; the gap luminosity by still-camera photography; and the observed time lag of flashover and probability distribution of the flashover were all investigated to analyze the breakdown mechanism.

The following points describe the salient conclusions.

(1) There is no difference of the 50% probability of flashover voltage between the spot illumination of the ultraviolet rays and the entire illumination on the cathode.

(2) Broad luminosity, observed in the case of the entire illumination on the cathode, has not been observed with spot illumination in air and N_2. Phenomena such as streamer disconnects in the middle of the gap, observed in the entire illumination in O_2, have not been observed in the case of the spot illumination.

(3) The minimum value of the probability distribution increases as the gap length increases. The calculated transit time of the electron to satisfy the conventional streamer criteria for

air, however, does not coincide with the probability distribution but is below the distribution.

(4) The probability distribution for O_2 is different from air and N_2. The distribution is narrow and the probability density does not depend on gap length under the experimental condition employed.

(5) On the basis of electron drift velocity and streamer velocity, the observed time lag of flashover of air can be explained by the conventional avalanche-to-streamer development theory.

References

1) L.B Loeb, Fundamental processes in Electrical Discharges in Gases. (John wiley and Sons, Inc, New York 1939).

2) J.M.Meek and J.D.Craggs, Electrical Breakdown of Gases (Oxford, Clarendon, 1953)

3) Y.Kawada, S.Shamoto and T.Hosokawa, Nanosecond-pulse breakdown of gas-insulated gaps, J.Appl.Phys.63, pp.1877-1881(1988)

4) K.Honda, On a streamer breakdown criterion of a uniform air gap, J.I.E.E.J.85. pp.116-123(1965).

5) H.Raether, Über den aufbau von gas entladungen. I

Z.Phys. 117, pp.375-398(1941)

6) S.Shamoto,

Generation of nanosecond-pulse and breakdown of gas-insulated gaps, M.Sc thesis of Nagoya Institute of Technology, pp. 102(1983).

Chapter IV Observation of Nanosecond-Pulse Breakdown of Gas-Insulated Gaps by Image Converter Camera*

1 Introduction

Breakdown phenomena of gas-insulated gaps with nanosecond pulses (rise times of 10.8 ns and pulse duration at half peak of 30 ns) were examined. In the previous articles,[1,2] to clarify the streamer formation and its development under the nanosecond impulse application, an examination of $P\ell$ (P:pressure; ℓ :gap length) versus flashover characteristics was carried out. Physical appearance, i.e. luminosity of a gap was examined by still-camera photography, and observed time lag of flashover and probability distribution of the time lag were also

* Accepted for publication and to be published on 15 January 1990 issue of the Journal of Applied Physics

examined to analyze the breakdown mechanism.

From scientific and technological points of view, the following three formulas[3,4] were referred to in the explanation of streamer criteria and the formative time lag of flashover.

(a) $\alpha/P=1.16\times10^{-4}(E/P-28.0)^2$

(b) $v_e=1.25\times10^7(E/P/40)^{1/2}$

(c) $\int_0^T \alpha \cdot v_e \, dt=20$

α is the ionization coefficient in cm^{-1}; P is the pressure in mmHg; E is the applied field in V/cm; and v_e is the electron drift velocity in cm/s; and t is the time in s.

These results and investigation have already been reported in the separate two articles.[1,2] The following points describe the salient conclusions stated in the articles.

(1) Under impulse voltage with half-peak width, 30ns, Paschen's law maybe applicable in air. This means that conventional avalanche-to-

streamer theory may be applicable to explain the breakdown mechanism.

(2) The minimum value of the probability distribution of time lag (time from the voltage application to flashover) increases as the gap length increases. The calculated transit time of the electron to satisfy the conventional streamer criteria for air (time from the start of the electron from the cathode surface to the streamer formation).however, does not coincide with the probability distribution but is beLow the distribution.

(3) On the basis of electron drift velocity and streamer velocity, the observed time lag of flashover of air can be explained by the conventional avalanche-to-streamer development theory.

These experimental and theoretical approaches lead to the following physical aspects on the growth of the avalanche and the development of stremer in spark breakdown.

One electron is emitted from the cathode by the irradiation of the weak ultraviolet rays. In the case of the ultrahigh-field gaps in these tests, the ionization coefficient, α ,as calculated from the formula (1), is so large that the growth of the avalanche can rapidly occur toward the anode. These electrons with the velocity of the

formula (2) travel at most 1 mm within several nanoseconds (at ℓ = 1 and 2 cm) after the impulse voltage application, and due to the ionization by collisions, the electron density ahead of the avalanche may exceed the order of 10^8, a number, as referred to in the formula (3), necessary to convert the avalanche into a streamer. In this stage, however, the streamer does not bridge over the gap so that the flashover of the gap has not been caused. This streamer develops toward the anode with a certain velocity and the flashover occurs when the gap is bridged over by the streamer.

In the breakdown mechanism of dc or impulse voltage application, the formative time lag is usually compared with the electron's transit time across the gap to analyze the breakdown mechanism[5]. The transient phenomena of the avalanche developing into streamer is negligibly small, compared with the duration of the voltage application so that the evaluation of the electron's transit time across the gap seems to be reasonable for that kind of breakdown under dc or impulse voltage

application.

In the case of the ultrahigh-field gaps in these tests, however, the physical phases such as the growth of the avalanche, the formation of a streamer and the development of the streamer into flashover is comparable to the same time order of the voltage duration so that each physical phase should be carefully examined to investigate the breakdown mechanism.

From these points of view, the time which is required from the voltage application to the occurrence of the flashover may be divided into

(a) the time in which the electrons emitted from the cathode propagate into the gap and form an avalanche that satisfies the streamer criteria.

(b) the time in which the streamer propagates toward the anode and connects the gap, causing the flashover.

The above mentioned physical models are deduced on the basis of the previous theoretical and experimental explanations.

As a follow on to previous experiments, to verify the above physical models i.e. the conventional avalanche-to-streamer

development theory by a visual method, physical appearance, i.e. luminosity of a gas in the gap was experimentally examined by an image converter camera. The observation of the luminosity in the gap obtained by the image converter camera clearly shows that the streamer starts on the surface of the cathode or in the vicinity of the cathode surface, irradiated by weak ultraviolet rays and develops toward the anode. The intensity of luminosity of the streamer , bridged over and connected between the cathode and the anode becomes stronger with time and finally the flashover occurs. This article reports the experimental results taken by the image converter camera and shows that the breakdown mechanism proposed by the author is consistent with the photographic evidence taken by the image converter camera.

2 APPARATUS

The diagram of this experimental circuit and data acquisition system is shown in Fig. 1. The high-voltage impulse generator used in this study is a coaxial Marx-type generator. Maximum output voltage is 130 kV and is set by the charging voltage on the Marx generator and its output resistor($CuSO_4$ solution). Two different electrode configurations were used in this experiment. Uniform test gaps are stainless-steel Rogowski-shaped electrodes with a diameter of 9 cm. Rod-plane nonuniform electrode system consists of the rod electrode (radius of curvature r=2.0 cm) and Rogowski-shaped electrode with a diameter of 9 cm. For the test, the stainless container in which the test gaps are located was evacuated to 10^{-5} Torr using rotary and diffusion pumps. Air was then backfilled into the container to the desired pressure. To minimize the fluctuations of the flashover voltage, as shown in Fig. 2, ultraviolet rays were continuously applied to the cathode surface through the 1 mm-diam. hole located in the center of the anode. Each shot was separated by 1-min intervals to allow the experiment to stabilize. The luminosity of a gas in the

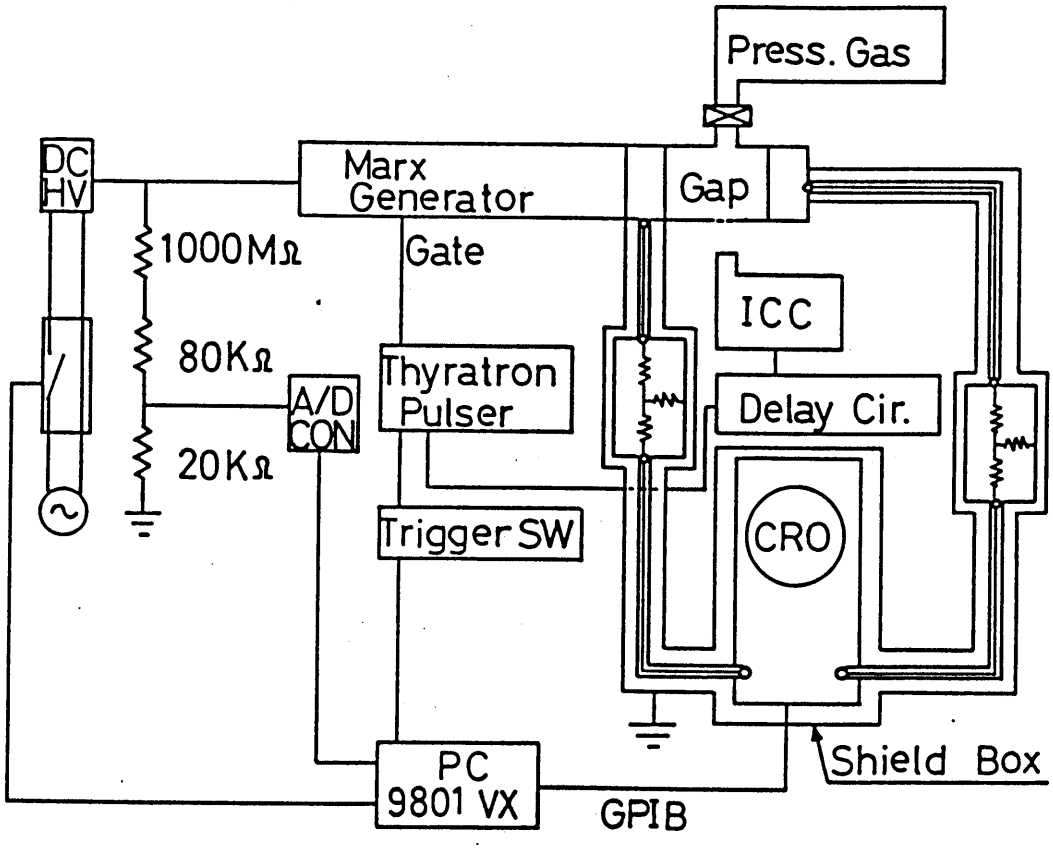

Fig. 1 Experimental circuit arrangement and data acquisition system

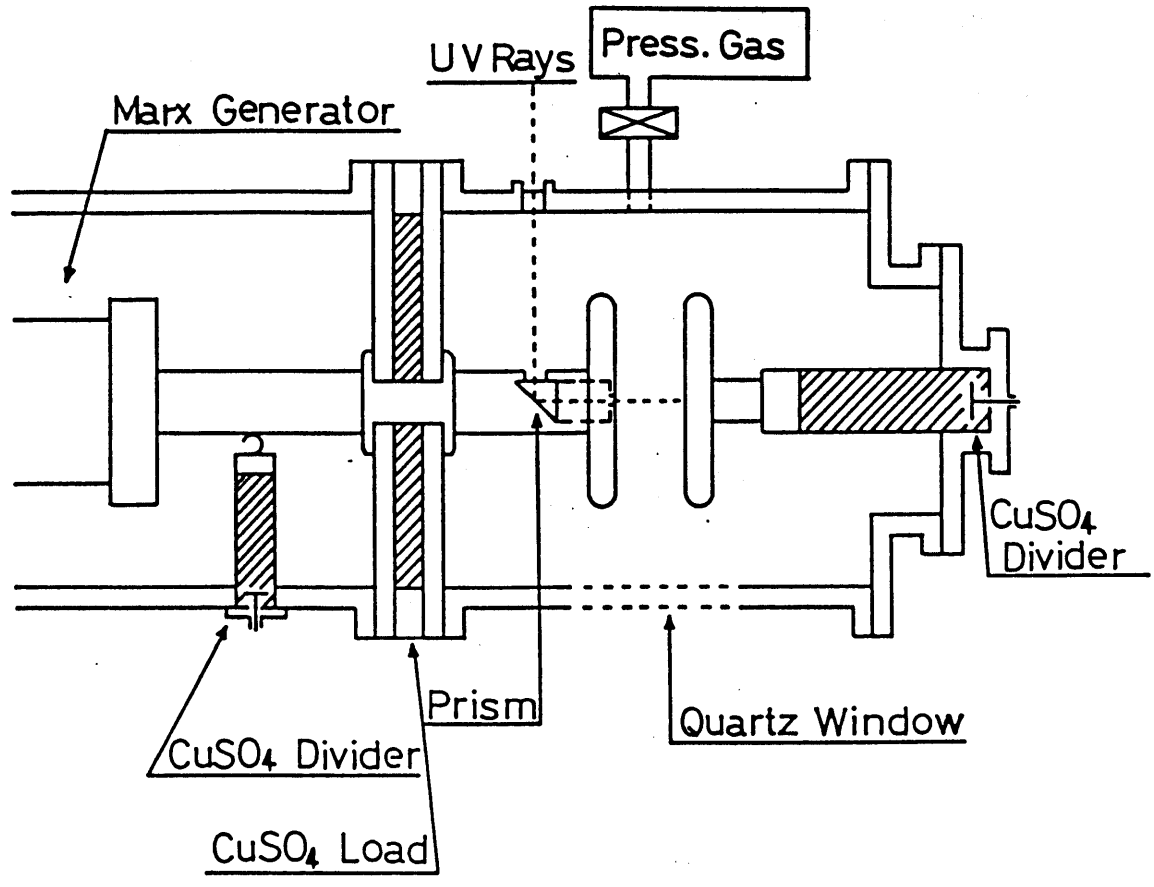

Fig. 2 Test gaps and illumination method of ultraviolet rays

gap was observed through the quartz window by the image converter camera (called hereafter ICC. IMACON 790 by JOHN HADLAND (P.I.) Ltd.), installed in a completely darkened room. Delay circuits were used to take a synchronization between the operation of the image converter camera and the triggering of the Marx generator. Measurements of waveforms of impulse voltages and currents are the same , referred to in our previous articles[1,2]. All experiments were carried out in air because published experimental data for physical coefficients of other gases such as O_2 and N_2 were insufficient to analyze the breakdown mechanism compared with published data for air. An impulse waveform used during this test is shown in Fig.3. Rise times of 10.8 ns and pulse durations at half peak of 30 ns are obtained.

3 EXPERIMENTAL RESULTS

The author will now describe the photographic evidence of the luminosity of a gas in the gap, taken by the ICC. Typical streak

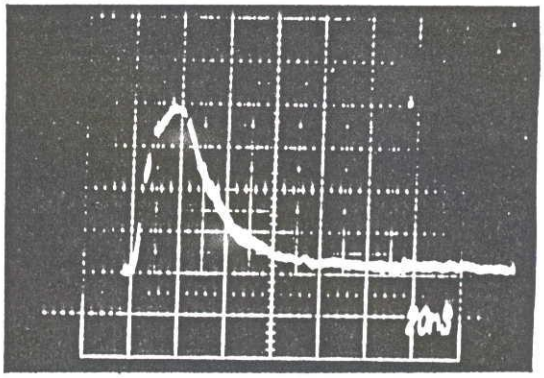

Fig. 3 Impulse waveform

photographs which show breakdown phenomena in air are shown in Figs.4 and 5. The discharge path of the breakdown by still-camera photography is also shown in the same figure.

A. Luminosity of a gas in a uniform field

Typical streak photograph observed in a uniform field is shown in Fig.4. The gap arrangement employed in this study is ℓ = 1 cm. The applied pressure in air is 1 atm. The applied voltage is 70 KV. The values stated in the figures are obtained from waveforms of the impulse voltages and currents, including the circuit system delays and show the time after the impulse voltage application[2]. It is observed in the Fig.4 that a white luminosity (called hereafter streamer) has started on the cathode surface several nanoseconds later after the impulse voltage application (an arrow shows the start of the streamer) and has reached the anode within four nanoseconds after its

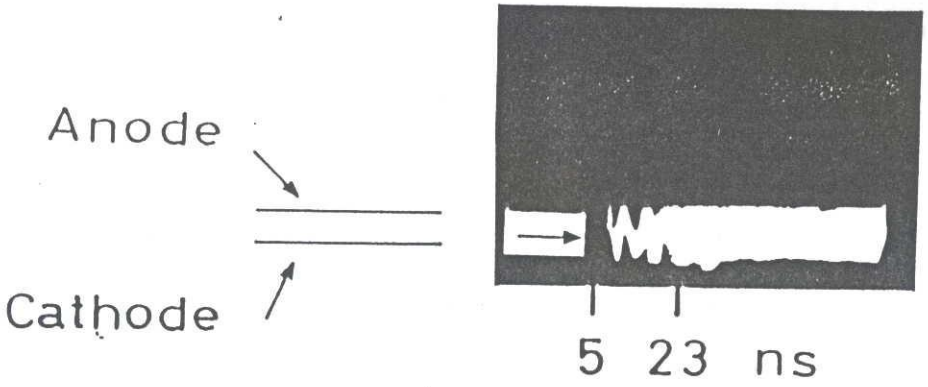

Fig. 4 Streak photograph in a uniform field

V=70 kV, P=1 atm, air, ℓ =1 cm.

initiation. After the anode directed streamer reaches the anode surface, another streamer(cathode directed streamer) has been observed to develop toward the cathode from the anode with the same velocity of the initial luminosity from the cathode surface. The author observes in the Fig.4 the following process; a streamer starts on the cathode surface, develops toward the anode, reaches the anode, and another streamer from the anode surface starts toward the cathode and reaches the cathode surface, this process repeats two times before spark and the intensity of the luminosity of the streamer becomes stronger as time passes. Each streamer velocity is 0.3×10^{8} cm/s. The flashover i.e. spark occurs 23 nanoseconds later after the impulse voltage application.

In uniform field gaps such as $\ell = 2$ cm, breakdown phenomena, similar to those in $\ell = 1$ cm were also observed in the ICC photography in air. In the still photography obtained in the breakdown, only a single spark channel is observed as shown in Fig.5 of the previous article[2] so that the cathode directed streamer seems to develop toward the cathode on the same streamer path initiated with the previous anode directed streamer.

B. Luminosity of a gas in a nonuniform field

A typical streak photograph which shows breakdown phenomena observed in a nonuniform field in air is shown in Fig.5. The discharge path of the breakdown observed in still-camera photography is also shown in the same figure to clear the gap configuration. The gap arrangement employed in this study is ℓ =3 cm and r=2 cm. The applied voltage is 130 KV. It is observed that a white luminosity has been formed on the surface of the cathode several nanoseconds later when the impulse voltage is applied to the gap. The luminosity develops toward the anode and the streamer has reached the anode 46 ns later after the impulse voltage is applied to the gap. The flashover (i.e. spark) does not occur at this time, 46 ns and 5 ns more is required to accomplish the flashover. The streamer velocity observed in the photograph is 0.56×10^8 cm/s. It is observed that the strong luminosity connects between the cathode and the anode in the still-camera photography. In such a gap arrangement with gap

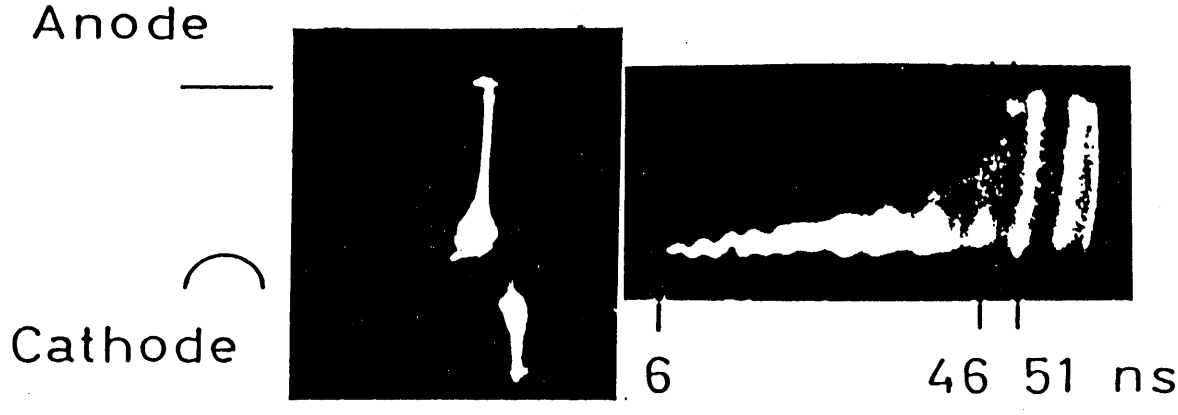

Fig. 5 Streak photograph in a nonuniform field

V=130 kV, P=1 atm, air, ℓ=3 cm, r=2 cm.

length, ℓ =3 cm, in a nonuniform field, a streamer can also be formed on the surface of the cathode or in the vicinity of the cathode within several nanoseconds and the streamer propagates toward the anode with the velocity of the order of 10^8 cm/s. In this gap condition, the streamer's return processes observed in the uniform field have not been detected yet in our experiments. Further experiments have already been started to investigate the breakdown phenomena in details.

As explained above, .in the case of the ultrahigh-field gaps with nanosecond pulses, a streamer is formed on the cathode surface or in the vicinity of the cathode and develops toward the anode. Several nanoseconds are required to accomplish the flashover i.e. spark after the anode directed streamer reaches the anode. In the uniform field gaps, another streamer is caused to start on the anode surface and propagates toward the cathode. The intensity of the luminosity becomes stronger as time passes and flashover occurs after repeating these streamer developing processes a few times.

4 DISCUSSION

The author has examined the luminosity of a gas in the gap with help of ICC to verify the author's proposed physical models i.e. conventional avalanche-to-streamer development theory. To clarify the breakdown characteristics of gas-insulated gaps in the atmospheric ga: of air by applying 30-ns impulse voltages, an examination of p ℓ versus flashover characteristics, luminosity of a gas in the gap by still-camera photography, observed time lag of flashover and probability distribution of the time lag have already been reported i the previous two separate articles[1,2]. On the basis of these experimental results, the author clarified the breakdown mechanism of the gas-insulated gaps and proposed the conventional avalanche-to-streamer development theory to explain the breakdown phenomena.
The main purpose of this third article in this series is to obtain photographic evidence which shows a luminosity of a gas in the gap by an optical method instead of the electrical methods employed in the previous experiments. As indicated in Figs.4 and 5, it is clearly

shown that the streamer starts on the cathode surface or in the vicinity of the cathode surface (the discrimination is very difficult due to halation of ICC photos) toward the anode with a velocity of the order of 10^8 cm/s within several nanoseconds after the impulse application. This means that in ultrahigh-field gaps, subjected to nanosecond pulses, streamer criteria can be satisfied in the place adjacent to the cathode surface.

On the other hand,, the author observed that the spark does not occur immediately even if the anode directed streamer, initiated on the cathode surface reaches the anode surface. A few return processes of the streamer are required to cause the spark between the cathode and the anode in the uniform field case. During these processes, the luminosity of the streamers becomes stronger as time passes. The author postulate that the formation of cathode spot causes the spark because sufficient electron emission from the cathode surface is required to supply energy into the plasma streamer with high conductivity. The phenomena, observed in the uniform field, such as an occurrence of a few return processes of the streamer before the spark and the flashover process detected in the nonuniform field are

very similar to those in the article[6]. Further investigation is required to clarify the flashover processes.

As discussed above in the case of the ultrahigh-field gaps subjected to nanosecond pulses, the conventional streamer theory may be applicable to the gap. The author believes that the proposed breakdown mechanism reported in the previous articles is consistent with the photographic evidence obtained by ICC.

5 CONCLUSION

Breakdown phenomena i.e. the luminosity of gas-insulated gaps with nanosecond pulses were examined by the image converter camera to verify the breakdown mechanism. The following points describe the salient conclusions:

(1) In the ultrahigh-field gaps, subjected to nanosecond pulses, the streamer can be formed on the cathode surface or in the vicinity of the cathode surface.

(2) The streamer develops toward the anode with a velocity of the order of 10^8 cm/s.

(3) To accomplish the flashover i.e. spark, several nanoseconds are required after the anode directed streamer reaches the anode surface.

(4) In the uniform field, another streamer is caused to start from the anode surface toward the cathode after the initial anode directed streamer reaches the anode. Sparks occur after these streamers repeat between the both electrodes a few times.

References

1. Y.Kawada. S.Shamoto. and T.Hosokawa,

Nanosecond-pulse breakdown of gas insulated gaps,

J.APPL Phys. 63. pp.1877-1881(1988)

2. Y.Kawada and T.Hosokawa,

Breakdown phenomena of gas-insulated gaps with nanosecond pulses,

J.APPL.Phys.65. pp.51-56(1989)

3. K.Honda,

On a streamer breakdown criterion of a uniform air gap,

J.I.E.E. Jpn.85, pp.116-123(1965)

4. H.Raether,

Über den aufbau von gas entladungen.

Z.Phys. 117, pp.375-398(1941)

5. Y.Kawada and T.Hosokawa,
Breakdown mechanism of a laser triggered spark gap in a uniform field gap,
J.APPL.Phys. 62, pp.2237-2242(1987)

6. I.Tsuneyasu, Y.Izawa, K.Nishijima and K.Watanabe,
DC breakdown process of negetive rod to plane gaps in atmospheric air,
Trans.IEE Jpn.108-A, pp.183-190(1988)

Chapter V Conclusions

The author has carried out research on breakdown phenomena in several kinds of gases, that were subjected to impulse voltages (10.8× 30 ns). The impulse voltages have an influence on the time of streamer formation and allowed investigating the transition from an electron avalanche to a streamer in addition to the flashover mechanism of gas-insulated gaps.

The following describes salient conclusions in addition to the waveform analysis of the coaxial Marx generator used in this test.

I Development and waveform analysis of a coaxial-type Marx generator

(1) The output impulse voltage of the CMG (coaxial-type Marx generator) can be analyzed by the distributed constant circuits, whose each stage forms a module.

(2) The reduction of the internal inductance existed in each module and the inductance in the last stage module with output terminals is required to increase the rise time of the impulse voltage.

(3) The reduction of the internal inductance existed in each module and the capacity of a charging ceramic capacitor in each module is required to obtain the impulse voltage with a short pulse duration. The reduction of the capacity of a charging ceramic capacitor is the most appropriate because it is difficult to change the value of the internal inductance existed in each module.

(4) The values of capacity of a spark gap in each stage, stray capacity between 2nd through 5th module and the container wall in each stage, and inductance in the last stage with output terminals should be as small as possible to reduce the harmonics in the impulse voltage.

(5) Current measurement can be made by the pick-up coil with a single turn.

II Nanosecond pulse breakdown of gas-insulated gaps

(1) Under impulse voltage with half peak width, 30 ns, Paschen's law may be applicable in air and N_2 at gap length, ℓ =1 and 2 cm. At ℓ = 3 cm, the 50% flashover voltage showed higher values than at ℓ = 1 and 2 cm.

Conventional avalanche-to-streamer theory may be applicable to explain the breakdown mechanism associated with ℓ =1 and 2 cm. Further investigation is required to explain the phenomena at ℓ = 3 cm.

(2) Under impulse voltage with half peak width, 30 ns, in O_2, the 50% flashover voltage showed different values at each gap length and Paschen's law may not be applicable to this gap. Including physical coefficient of electron attachment, further investigation is required to analyze the phenomena.

(3) Under impulse voltage with half peak width, 74 ns, Paschen's law may be applicable in air, N_2 and O_2 at each gap length.

(4) In the case of the ultra high field gaps in these tests, the author showed that an electron emitted from the cathode satisfied

streamer criteria within developing distance of the electron, 1.8 mm and can develop into streamer, causing flashover.

Ⅲ Breakdown phenomena of gas-insulated gaps with nanosecond pulses

(1) There is no difference of the 50% probability of flashover voltage under the methods between the spot illumination of the ultra-violet rays and the entire illumination on the cathode.

(2) Broad luminosity, observed in the case of the entire illumination on the cathode, has not been observed in the spot illumination in air and N_2.

Such phenomena that streamer disconnects in the middle of the gap, observed in the entire illumination in O_2, have not been observed in the case of the spot illumination.

(3) Minimum value of the probability distribution increases as the gap length increases. The calculated transit time of the electron to satisfy the conventional streamer criteria for air, however, does

not coincide with the probability distribution but places beyond distribution at the lower side.

(4) The probability distribution for O_2 is quite different from air a N_2. The distribution is narrow and the probability density does n depend on gap length under the experimental condition employed.

(5) On the basis of electron drift velocity and streamer velocity, th observed time lag of flashover of air can be explained by the conventional avalanche-to-streamer development theory.

IV Observation of nanosecond-pulse breakdown of gas-insulated gaps by Image Converter Camera

(1) In the ultrahigh-field gaps, subjected to nanosecond pulses, the streamer can be formed on the cathode surface or in the vicinity the cathode surface.

(2) The streamer develops toward the anode with a velocity of the ord of 10^8 cm/s.

(3) To accomplish the flashover, i.e., spark, several nanoseconds are

required after the anode directed streamer reaches the anode surface.

(4) In the uniform field, another streamer is caused to start from the anode surface toward the cathode after the initial anode directed streamer reaches the anode. Spark may occur after these streamers repeat between the both electrodes a few times.

Acknowledgment

The author wishes to express my cordial thanks to professor, Dr. T. Hosokawa, Department of Electrical and Computer Engineering, Nagoya Institute of Technology, Professor, Dr. T. Iwazumi, Department of Electrical and Computer Engineering, Nagoya Institute of Technology, Professor, Dr. Y. Tsunehiro , Department of Electrical and Computer Engineering, Nagoya Institute of Technology, Professor, Dr. M. Hayashi Department of System's Engineering, Nagoya Institute of Technology, Professor Dr. N. Matsui, Department of Electrical and Computer Engineering, Nagoya Institute of Technology and Dr. Yasunori Miyoshi, professor emeritus of Nagoya Institute of Technology for the advice.

The author also wishes to express my cordial thanks to the group members, Dr. S. Takeda, professor emeritus of Nagoya University, professor, Dr. H. Sugai, Department of Electrical Engineering, Nagoya University and associate professor, Dr. M. Sekiya, Department Daido Institute of Technology on gaseous discharge, whose meetings have been held two times every year to show the member's latest research activities.

The author also wishes to express my cordial thanks to Dr. M. Cernak (who is, at present, researcher of Nagoya Institute of Technology), Institute of Physics and Biophysics, Comenius University, Czechoslovakia, Mr. B. Aissa (who is, at present, researcher of Nagoya Institute of Technology), Algeria and the group members on the gaseous discharge in our laboratory.

List of articles published

(1) Y. Kawada, S. Suzuki, T. Hosokawa, and Y. Miyoshi,
Breakdown mechanism of a laser triggered spark gap in a nonuniform field [I]
Trans. IEE Jpn. 95-A, pp. 416-422 (1975) (in Japanese)

(2) Y. Kawada, T. Hosokawa, and Y. Miyoshi,
Breakdown mechanism of a laser triggered spark gap in a nonuniform field [II] ,
Trans. IEE Jpn. 99-A, pp. 39-46 (1979) (in Japanese)

(3) Y. Fukuoka, Y. Kawada, Y. Yoneda, T. Hosokawa, and Y. Miyoshi,
Breakdown mechanism of a laser triggered spark gap in a nonuniform field [III] ,
Trans. IEE Jpn. 101-A, pp. 595-602 (1981) (in Japanese)

(4) Y. Kawada, and T. Hosokawa,
Breakdown mechanism of a laser triggered spark gap in a uniform field gap,
J. Appl. Phys. 62, pp.2237-2242(1987)

(5) Y. Kawada, S. Shamoto, and T. Hosokawa
Nanosecond-pulse breakdown of gas-insulated gaps,
J. Appl. Phys. 63, pp.1877-1881(1988)

(6) Y. Kawada, and T. Hosokawa,
Breakdown phenomena of gas-insulated gaps with nanosecond pulses,
J. Appl. Phys. 65, pp.51-56(1989)

(7) Y. Kawada, and T. Hosokawa
Observation of nanosecond-pulse breakdown of gas-insulated gaps by image converter camera,
J. Appl. Phys. accepted for publication and to be published in 15 January 1990 issue